Resource-Based Time and Cost Prediction in Project Networks: From Statistical Modeling to Graph Neural Networks

Reza Mirjalili, Behrad Barghi, Shahram Shadrokh Sikari, November 20, 2025

Abstract

Accurate prediction of project duration and cost remains one of the most challenging aspects of project management, particularly in resource-constrained and interdependent task networks. Traditional analytical techniques such as the Critical Path Method (CPM) and Program Evaluation and Review Technique (PERT) rely on simplified and often static assumptions regarding task interdependencies and resource performance. This study proposes a novel **resource-based predictive framework** that integrates network representations of project activities with **Graph Neural Networks (GNNs)** to capture structural and contextual relationships among tasks, resources, and time–cost dynamics. The proposed model represents the project as a **heterogeneous activity–resource graph**, where nodes denote activities and resources, and edges encode temporal and resource dependencies.

We evaluate multiple learning paradigms—including **GraphSAGE** and **Temporal Graph Networks (TGN)**—on both synthetic and benchmark project datasets. Experimental results indicate that the proposed GNN framework achieves an average 23–31% reduction in Mean **Absolute Error (MAE)** compared to traditional regression and tree-based methods, while improving the coefficient of determination (R^2) from ≈ 0.78 to ≈ 0.91 for large and complex project networks. Furthermore, the learned embeddings provide interpretable insights into resource bottlenecks and critical dependencies, enabling explainable and adaptive scheduling decisions.

Keywords: Project Management, Resource-Based Prediction, Graph Neural Networks, Time–Cost Estimation, Machine Learning

1 Introduction

Accurate prediction of project duration and cost remains one of the most persistent challenges in project management and operations research. Despite decades of methodological progress—from deterministic scheduling techniques such as the Critical Path Method (CPM) [32] and Program Evaluation and Review Technique (PERT) [45] to stochastic and simulation-based models [24, 61]—real-world projects continue to deviate systematically from planned baselines. Large-scale meta-analyses across construction, infrastructure, IT, and R&D sectors reveal persistent patterns of cost and schedule overruns, often exhibiting heavy-tailed distributions [18, 19]. These empirical observations underscore the presence of complex, nonlinear, and interdependent dynamics that classical analytical models struggle to capture.

Motivation. Traditional approaches to project time and cost estimation rely on activity-centric models with static assumptions about productivity and independence among tasks. The fundamental premise of CPM—that project duration is determined by a fixed critical path computed from deterministic activity durations—has proven inadequate for modern project environments characterized by resource constraints, dynamic interdependencies, and adaptive management interventions [8]. In reality, project outcomes emerge from evolving interactions among three key subsystems: resources (human, material, and financial), managerial policies (planning, control, and adaptation), and environmental factors (market conditions, technological change, and external disruptions) [42].

Resource performance, in particular, exhibits significant variability driven by learning effects [28], fatigue and burnout [37], skill heterogeneity, team dynamics, and collaboration patterns [16]. When multiple resources work on interdependent activities, performance variations propagate through the project network, creating cascading effects that amplify uncertainty [60]. Furthermore, resource contention—competition for shared resources across parallel activities—introduces scheduling conflicts and delays that cannot be captured by independence assumptions underlying PERT [39].

^{*}Department of Industrial Engineering, University of Houston, Corresponding author: Shadrokh@sharif.edu

 $^{^\}dagger \mbox{Department}$ of Industrial Engineering, Rochester Institute of Technology

[‡]Department of Industrial Engineering, Sharif University of Technology

The increasing availability of granular project execution data—ranging from resource allocation logs and progress updates to cost accruals and change orders—offers unprecedented opportunities for data-driven forecasting. Modern enterprise project management systems, Building Information Modeling (BIM) platforms, and collaborative software development tools generate rich temporal records of project evolution [30]. However, most predictive tools in practice, such as regression-based earned value management (EVM) [41] or Monte Carlo risk analysis [57], remain aggregate in nature and fail to exploit the relational structure inherent in project networks.

Research gap. A comprehensive review of existing literature (detailed in Section 2) reveals a fundamental tension between two complementary modeling paradigms. On one hand, analytical models rooted in operations research—including stochastic PERT [45], resource-constrained project scheduling [4], and system dynamics simulations [43]—provide mechanistic interpretability and can incorporate domain knowledge through explicit causal relationships. These models enable what-if analysis and scenario planning but typically rely on simplified parametric assumptions (e.g., beta-distributed durations, linear resource consumption) that may not hold in practice. Moreover, they require extensive manual specification of probability distributions, correlation structures, and functional forms, limiting their adaptability to new project contexts.

On the other hand, recent applications of machine learning to project prediction—employing neural networks [54], tree-based ensembles [11], and time series models [15]—have demonstrated superior predictive accuracy by learning nonlinear relationships directly from data. However, these approaches typically treat each activity or project as an independent observation, ignoring the underlying network topology of precedence and resource dependencies. By discarding structural information, they fail to capture how local performance variations propagate through the project graph to influence downstream activities and overall project outcomes. Furthermore, most machine learning models provide point predictions without quantifying uncertainty, limiting their utility for risk-informed decision making [33].

Critically, no prior work has developed an integrated framework that simultaneously:

- 1. Models projects as heterogeneous graphs encoding both precedence and resource relationships,
- 2. Links stochastic resource performance to activity and project outcomes through explicit propagation mechanisms,
- 3. Learns complex, nonlinear dependencies from data while maintaining structural consistency with project networks,
- 4. Quantifies predictive uncertainty at activity and project levels to support risk assessment,
- 5. Adapts predictions dynamically as projects evolve using Bayesian online learning,
- 6. Guides efficient data collection through active learning informed by network topology.

This gap is particularly significant given the natural fit between project networks and modern graph neural network (GNN) architectures [25, 36], which have achieved state-of-the-art performance across diverse domains—from molecular property prediction [22] to social network analysis [17]—by learning representations that jointly encode node features and relational structure.

Objective and contributions. This research develops a unified Resource-Based Modeling (RBM) and Graph Neural Network (GNN) framework that bridges analytical interpretability with adaptive, data-driven learning. The proposed approach represents projects as heterogeneous graphs where nodes denote activities and resources, and edges encode temporal precedence, resource assignments, and collaboration patterns. Resource performance is modeled as a latent stochastic process that influences activity durations and costs through explicit functional relationships derived from productivity theory. A dynamic GNN learns to predict activity-level outcomes while respecting project-level constraints through a hierarchical loss formulation incorporating a differentiable critical path term.

The key contributions of this work are:

- 1. Hierarchical resource-based model (RBM): A formal stochastic framework linking micro-level resource efficiency distributions to activity durations and costs, with explicit propagation to project makespan and total cost. The model incorporates realistic features including parallel/serial/mixed activity structures (Eq. (8)), convex time-cost tradeoffs (Eq. (14)), and variance propagation under dependency structures (Eq. (13)).
- 2. **Dynamic heterogeneous GNN architecture:** A graph neural network tailored to project networks with multiple node types (activities, resources) and relation types (precedence, assignment, collaboration). The architecture includes:

- Relation-specific message passing (Eqs. (18a)–(18c)) capturing differential influence of precedence vs. resource dependencies,
- Temporal graph network variant (Eqs. (19a)–(19c)) with GRU-based memory for non-stationary project dynamics,
- Heteroscedastic prediction heads (Eqs. (20)–(21)) jointly estimating means and uncertainties for duration and cost.
- 3. **Bayesian online updating mechanism:** A Kalman filtering framework (Eqs. (29a)–(29c)) for real-time refinement of resource efficiency distributions as activities complete and performance data become available. This enables adaptive forecasting that improves accuracy as projects progress and reduces reliance on initial parameter specifications.
- 4. Active measurement allocation strategy: A principled approach (Eq. (30)) combining predicted uncertainty (activity-level variance) with graph-theoretic criticality metrics (betweenness centrality, critical path proximity) to prioritize which activities should be monitored closely. This addresses the practical constraint of limited observation budgets in large projects.
- 5. **Hierarchical consistency loss:** A novel training objective (Eqs. (25)–(28)) enforcing coherence between activity-level predictions and project-level aggregates through a differentiable soft critical path constraint. This ensures that learned embeddings respect fundamental project scheduling logic while leveraging data-driven flexibility.
- 6. Comprehensive empirical evaluation: Rigorous experiments on synthetic project networks (spanning |V|=20–500 activities) and established benchmarks (PSPLIB, NASA93, COCOMO II, Desharnais) demonstrating:
 - 23–31% reduction in Mean Absolute Error (MAE) compared to best non-graph baselines,
 - Improvement in coefficient of determination from $R^2 \approx 0.78$ to $R^2 \approx 0.91$,
 - Superior uncertainty calibration (Expected Calibration Error <4%) and 90% prediction interval coverage (> 89%),
 - Near-linear scalability in project size with neighbor-sampling mini-batch training.

Research significance. By integrating resource-based analytical reasoning with graph-based deep learning, this study advances both the theory and practice of project performance forecasting. The hybrid framework preserves the mechanistic interpretability of operations research models—enabling practitioners to understand why predictions change and which resources or activities drive risk—while harnessing the representational power and adaptive learning capabilities of neural networks. This synergy addresses a critical need in project management: moving beyond static, one-time baseline estimates toward continuous, probabilistic forecasts that evolve with project execution.

The practical implications are substantial. Project managers can leverage the proposed system to: (1) identify high-risk activities and resource bottlenecks early in execution through uncertainty quantification; (2) allocate limited monitoring and control resources efficiently via active learning; (3) perform scenario analysis and dynamic replanning based on updated forecasts as new information arrives; and (4) communicate project status and risks to stakeholders using interpretable graph visualizations that reveal critical dependencies and performance drivers.

From a methodological perspective, this work demonstrates that domain-specific inductive biases—embodied in the heterogeneous graph construction, hierarchical loss formulation, and Bayesian update mechanisms—are essential for effective application of deep learning to project management. Purely data-driven approaches that ignore project structure and scheduling constraints fail to generalize across project scales and configurations, as evidenced by our ablation studies. The proposed framework thus establishes a template for developing physics-informed or logic-informed neural networks in other domains characterized by structured interdependencies and aggregate-level constraints.

Paper structure. The remainder of this paper is organized as follows: Section 2 reviews prior work in stochastic project modeling, machine learning for project prediction, graph neural networks, and Bayesian inference for dynamic systems, positioning our contributions within this landscape. Section 3 presents the Resource-Based Model formulation and extends it into the proposed GNN architecture with detailed specifications of message passing, temporal dynamics, loss functions, and learning algorithms. Section 4 describes the experimental design, including synthetic data generation protocols, benchmark datasets, baseline implementations, and comprehensive evaluation metrics, followed by presentation and analysis of results. Section 5 concludes with a synthesis of

findings, discussion of limitations, and directions for future research. Supplementary materials in the Appendix provide complete hyperparameter specifications and reproducibility protocols.

Paper structure. The remainder of this paper is organized as follows: Section 2 reviews prior work in stochastic project modeling, Bayesian learning, and graph neural networks. Section 3 presents the proposed Resource-Based Model and hybrid Bayesian–GNN methodology. Section 4 describes the experimental design and evaluation, followed by concluding remarks in Section 5.

2 Literature Review

2.1 Classical Project Scheduling and Uncertainty Modeling

The foundations of project scheduling theory were established through deterministic network techniques. The Critical Path Method (CPM) [32] and the Program Evaluation and Review Technique (PERT) [45] introduced network-based representations of project activities with precedence constraints. CPM assumes deterministic durations and identifies the longest path through the network as the critical constraint on project completion. PERT extends this by modeling activity durations as random variables following beta distributions and approximating project makespan via the central limit theorem.

Despite their widespread adoption, classical PERT exhibits systematic biases in estimating project completion times [44]. The assumption of path independence—that critical path variability alone determines project risk—fails when activities share common resources or when multiple near-critical paths exist [60]. Subsequent analytical refinements have addressed some limitations: moment-matching methods [51], conditional expectation approaches [14], and closed-form bounds on makespan distributions under specific network topologies [38].

Stochastic project modeling. Modern stochastic models recognize that uncertainty arises from resource performance variability, scope changes, and external disruptions rather than merely parametric activity duration distributions [61]. Resource-constrained project scheduling problems (RCPSP) [4,39] explicitly model limited resource availability and allocation trade-offs. However, most RCPSP formulations assume deterministic resource productivities and focus on schedule optimization rather than forecasting.

Monte Carlo simulation has become the de facto standard for practical uncertainty analysis [57], enabling arbitrary distributional assumptions and capturing complex dependencies. Yet simulation-based approaches suffer from computational cost, require extensive parametric specifications, and do not inherently learn from historical data [24]. Bayesian methods [16] offer a principled framework for updating beliefs as projects progress, but typically assume simplified parametric forms that may not capture real-world nonlinearities.

2.2 Resource-Based and System Dynamics Approaches

An emerging paradigm shifts focus from activity-centric to resource-centric modeling. The Design Structure Matrix (DSM) [8, 16] and related techniques capture task interdependencies through information flows and resource sharing. These models reveal that rework cycles, communication delays, and resource contention create feedback loops that classical CPM cannot represent [20].

System dynamics models [42, 43] simulate project evolution as continuous stock-and-flow processes, incorporating learning curves, fatigue effects, and workforce dynamics. While these models capture emergent behavior and policy feedback, they require detailed causal loop diagrams and differential equations that are difficult to calibrate from data [47]. Moreover, they typically operate at aggregate rather than activity-specific granularity, limiting their utility for detailed scheduling.

2.3 Machine Learning in Project Management

Recent years have witnessed growing interest in applying machine learning to project prediction tasks. Early work focused on regression-based earned value management (EVM) forecasting [34,41], using linear or polynomial models to extrapolate cost and schedule performance indices. While simple and interpretable, these methods ignore task-level dependencies and assume stationary project dynamics.

More sophisticated approaches employ tree-based ensembles [11,15] and neural networks [54] for duration and cost prediction. Wauters and Vanhoucke [59] use artificial neural networks to predict project completion time based on baseline schedules and resource profiles. Ballesteros-Pérez et al. [3] apply machine learning to estimate tender success probability in construction projects. However, these studies treat each activity or project as an independent observation, failing to exploit the relational structure inherent in project networks.

Deep learning for temporal and relational data. The advent of deep learning has enabled modeling of complex, high-dimensional relationships. Recurrent neural networks (RNNs) and Long Short-Term Memory (LSTM) networks [26] have been applied to sequential project data [10], capturing temporal dependencies in resource allocation and progress updates. Attention mechanisms [55] further allow models to focus on salient events or activities within long project histories.

Convolutional neural networks (CNNs) have been used for pattern recognition in Gantt charts and schedule matrices [30], treating projects as images. While innovative, these approaches discard the explicit graph topology of precedence and resource networks, instead relying on spatial inductive biases suited to grid-structured data.

2.4 Graph Neural Networks and Relational Learning

Graph Neural Networks (GNNs) [36, 49] provide a natural framework for learning from graph-structured data. By iteratively aggregating information from neighboring nodes, GNNs learn representations that encode both node features and structural context. Graph Convolutional Networks (GCNs) [36], GraphSAGE [25], and Graph Attention Networks (GATs) [56] have achieved state-of-the-art performance in domains ranging from social network analysis [17] to molecular property prediction [22].

Heterogeneous GNNs [50,58] extend this paradigm to graphs with multiple node and edge types, enabling differentiated message passing along distinct relation types. Temporal graph networks [48, 62] incorporate time-varying dynamics, updating node representations as events occur—a natural fit for project execution where activities complete and resources update over time.

Despite their success in other domains, GNNs remain underexplored in project management. Preliminary work [64] applies GCNs to software defect prediction in development projects, demonstrating that dependency graphs improve accuracy over tabular baselines. However, no prior study has developed a comprehensive GNN framework for joint time-cost prediction with uncertainty quantification and Bayesian resource-performance updating.

2.5 Bayesian Inference and Active Learning in Projects

Bayesian methods have a long history in project control. Bayesian updating of PERT parameters [31] and dynamic Bayesian networks for project risk assessment [27,63] demonstrate the value of probabilistic reasoning. Kalman filtering and particle filtering [35] enable real-time state estimation for project tracking, though most implementations assume linear Gaussian dynamics.

Active learning [52] addresses data scarcity by intelligently selecting which observations to acquire. In project contexts, measurement allocation—deciding which activities to monitor closely—balances information gain against observation cost [23]. Graph-based active learning [9] leverages network structure to prioritize samples in high-uncertainty or topologically critical regions, but has not been integrated with GNN-based project prediction.

2.6 Research Gap and Positioning

This review reveals a clear gap: existing analytical models offer interpretability but lack adaptability and data-driven learning, while machine learning approaches provide predictive power but ignore network structure and physical constraints. No prior work integrates:

- Resource-based stochastic models with explicit dependency propagation,
- Graph neural networks that respect project network topology,
- Bayesian online learning for adaptive resource-performance estimation,
- Active measurement allocation guided by topological criticality,
- Hierarchical consistency between activity- and project-level predictions.

Our proposed framework addresses this gap by unifying analytical resource-based reasoning with graph-based deep learning, creating a hybrid system that is simultaneously interpretable, adaptive, and scalable. This positions our work at the intersection of operations research, machine learning, and project management science.

3 Methodology

3.1 System Definition and Modeling Scope

We model a project as a complex system comprising three interacting domains: management policies (\mathcal{M}) , resource capabilities (\mathcal{R}) , and environmental conditions (\mathcal{E}) . While all three domains

influence project outcomes, full joint modeling is computationally intractable for large-scale systems [61]. Following the principle of parsimony and supported by empirical evidence that resource variability dominates schedule uncertainty [42], we focus on \mathcal{R} as the primary stochastic component.

Project network representation. The project is represented as a directed acyclic graph (DAG) G=(V,E) where nodes $i\in V$ correspond to activities and directed edges $(i,j)\in E$ encode precedence constraints. This representation aligns with classical CPM/PERT formulations [32] but is extended to incorporate resource-activity assignments and resource collaboration structures. Let \mathcal{P} denote the set of all paths from source to sink nodes in G; the critical path is $p^* = \arg \max_{p \in \mathcal{P}} \sum_{i \in p} T_i$ where T_i is the duration of activity i.

Each activity i requires a subset of resources $A_i \subseteq \mathcal{R}$. Resource j contributes work quantity $q_{i,j}$ (measured in person-hours, machine-hours, or appropriate units) to complete activity i. The distinction between assigned resources A_i and total resource pool \mathcal{R} allows modeling of resource contention and allocation flexibility.

Resource Performance Modeling

Traditional project models assume static, deterministic resource productivities. In reality, resource performance varies due to learning effects [28], fatigue [37], environmental factors, and inter-resource collaboration dynamics [8]. We define resource efficiency $R_{i,j}$ as the ratio of realized to standard productivity:

$$R_{i,j} = \frac{U_{i,j}^r}{U_{i,j}^s} \tag{1}$$

where $U_{i,j}^s$ represents the baseline or planned utilization rate (e.g., lines of code per day for software development, cubic meters per hour for excavation) and $U_{i,j}^r$ is the actual realized rate. The efficiency ratio satisfies:

- $R_{i,j} > 1$: overperformance relative to baseline (faster completion)
- $R_{i,j} = 1$: performance matches plan
- $R_{i,j} < 1$: underperformance (slower than expected)

Stochastic performance distribution. For activity i, the efficiency vector $R_i = [R_{i,j}]_{j \in A_i}$ is modeled as a random vector drawn from a parametric distribution:

$$R_i \sim F_i(M_i, \Sigma_i, \Theta_i)$$
 (2)

where $M_i \in \mathbb{R}^{|A_i|}$ is the mean vector, $\Sigma_i \in \mathbb{R}^{|A_i| \times |A_i|}$ is the covariance matrix capturing correlations among resources working on the same activity, and Θ_i represents higher-order moments (e.g., skewness, kurtosis) if non-Gaussian distributions are used.

The choice of distribution family depends on empirical characteristics:

- Gaussian: appropriate when efficiency reflects aggregated effects of many small independent factors (central limit theorem justification)
- Log-normal: enforces positivity and captures right-skewed distributions common in productivity data [1]
- Beta: bounded support [0,1] or rescaled [a,b] suitable when efficiency has natural bounds

Bayesian updating mechanism. As activities complete and performance data become available, we update resource efficiency parameters using Bayesian filtering. For resource j, the posterior mean and variance evolve as:

$$\hat{\mu}_j^{(t+1)} = (1 - \alpha_t)\hat{\mu}_j^{(t)} + \alpha_t \overline{R_{i,j}^{(t)}}$$
(3)

$$\hat{\mu}_{j}^{(t+1)} = (1 - \alpha_{t})\hat{\mu}_{j}^{(t)} + \alpha_{t} \overline{R_{i,j}^{(t)}}$$

$$\hat{\sigma}_{j}^{2(t+1)} = (1 - \alpha_{t})\hat{\sigma}_{j}^{2(t)} + \alpha_{t} \operatorname{Var}(R_{i,j}^{(t)})$$
(3)

where $R_{i,j}^{(t)}$ is the observed mean efficiency for resource j in completed activities up to time t, and $\alpha_t \in (0,1)$ is the learning rate controlling the weight given to new observations versus prior beliefs. The learning rate can be constant (exponential smoothing) or time-varying (e.g., $\alpha_t = 1/(t+1)$ for sample averaging, or adaptive based on observation reliability).

This update rule corresponds to a Kalman filter in the Gaussian case [29] or a moment-matching approximation for non-Gaussian distributions. When observations are sparse or noisy, one can incorporate observational uncertainty σ_{obs}^2 into the update:

$$\alpha_t = \frac{\hat{\sigma}_j^{2(t)}}{\hat{\sigma}_j^{2(t)} + \sigma_{obs}^2/n_t} \tag{5}$$

where n_t is the number of observations at time t.

Duration and Cost Formulas

Given resource efficiency $R_{i,j}$, the realized productivity of resource j on activity i is:

$$p_{i,j} = R_{i,j} p_j^s \tag{6}$$

where p_j^s is the standard (baseline) productivity rate. The time required for resource j to complete its portion of activity i is then:

$$t_{i,j} = \frac{q_{i,j}}{p_{i,j}} = \frac{q_{i,j}}{R_{i,j}p_i^s} \tag{7a}$$

$$t_{i,j} = \frac{q_{i,j}}{p_{i,j}} = \frac{q_{i,j}}{R_{i,j}p_j^s}$$

$$C_{i,j} = c_j t_{i,j} = c_j \frac{q_{i,j}}{R_{i,j}p_j^s}$$
(7a)

where c_j is the cost rate (e.g., dollars per hour) for resource j. Equation (7b) captures the key insight that lower efficiency $(R_{i,j} < 1)$ increases both duration and cost proportionally.

Activity-level aggregation. When multiple resources work on activity i, their individual durations $\{t_{i,j}\}_{j\in A_i}$ must be composed into a single activity duration T_i . The aggregation depends on the activity structure (AS):

$$T_i = \lambda_i \sum_{j \in A_i} t_{i,j} + (1 - \lambda_i) \max_{j \in A_i} t_{i,j}$$
(8)

where $\lambda_i \in [0,1]$ governs the degree of parallelism:

- $\lambda_i = 1$: serial activity—resources work sequentially (e.g., design followed by review)
- $\lambda_i = 0$: fully parallel activity—resources work simultaneously and activity completes when the slowest finishes (e.g., independent testing teams)
- $\lambda_i \in (0,1)$: mixed activity—partial parallelism with coordination overhead

This formulation generalizes the min-max models of parallel tasks [60] and additive models of sequential tasks into a unified convex combination. In practice, λ_i can be estimated from historical data or specified based on workflow analysis.

Total activity cost aggregates linearly:

$$C_i = \sum_{j \in A_i} C_{i,j} = \sum_{j \in A_i} c_j \frac{q_{i,j}}{R_{i,j} p_j^s}$$
(9)

Project-level metrics. Project makespan follows critical path logic [32]. Let F_i denote the finish time of activity i under a feasible schedule respecting precedence constraints. The makespan is:

$$T_{\text{proj}} = \max_{i \in V} F_i = \max_{p \in \mathcal{P}} \sum_{i \in p} T_i \tag{10}$$

The second equality holds when activities start as soon as their predecessors finish (earliest start schedule). Project cost includes activity costs plus fixed overhead:

$$C_{\text{proj}} = \sum_{i \in V} \sum_{j \in A_i} C_{i,j} + C_{\text{overhead}}$$
(11)

Variance propagation. When resource efficiencies are stochastic, activity durations and costs become random variables. Under the assumption of independence among $R_{i,j}$ (or conditional independence given resource latent states), we can derive approximate moments. For activity duration expectation:

$$\mathbb{E}[T_i] \approx \lambda_i \sum_{j \in A_i} \frac{q_{i,j}}{p_j^s} \mathbb{E}\left[\frac{1}{R_{i,j}}\right] + (1 - \lambda_i) \max_{j \in A_i} \frac{q_{i,j}}{p_j^s \mu_j}$$
(12)

For log-normal $R_{i,j} \sim \mathcal{LN}(\mu_j, \sigma_j^2)$, we have $\mathbb{E}[1/R_{i,j}] = \exp(-\mu_j + \sigma_j^2/2)$. More generally, using a second-order Taylor expansion around $R_{i,j} = \mu_j$:

$$\mathbb{E}[T_i] \approx \sum_{j \in A_i} \frac{q_{i,j}}{p_j^s \mu_j} \left(1 + \frac{\sigma_j^2}{\mu_j^2} \right) \tag{13}$$

This shows that variance in resource efficiency increases expected duration—a manifestation of Jensen's inequality for convex functions [61].

3.4 Stochastic Time-Cost Tradeoff

Classical CPM assumes a linear time-cost tradeoff: reducing activity duration by adding resources increases cost linearly [32]. In reality, the relationship is often convex due to diminishing returns and coordination overhead [53]. We model activity cost as a convex function of target duration:

$$C_i(T_i) = C_i^{\min} + a_i [e^{b_i(T_i^N - T_i)} - 1], \quad a_i, b_i > 0$$
(14)

where T_i^N is the normal (uncrushed) duration, C_i^{\min} is the minimum direct cost, and (a_i, b_i) control the curvature. As T_i decreases (crashing), cost increases exponentially; as $T_i \to T_i^N$, cost approaches C_i^{\min} .

The project cost frontier is obtained by solving:

$$\min_{\{T_i\}} \sum_{i \in V} C_i(T_i) \quad \text{s.t.} \quad T_{\text{proj}} \le T_{\text{max}}$$
(15)

This nonlinear program can be solved via convex optimization methods [7] when $C_i(\cdot)$ are convex. In our stochastic setting, we replace deterministic durations with expected values or quantiles (e.g., 90th percentile makespan target).

3.5 Graph Neural Network Architecture

3.5.1 Heterogeneous Graph Construction

The project is represented as a heterogeneous graph $\mathcal{G} = (\mathcal{V}, \mathcal{E}, \mathcal{T}_V, \mathcal{T}_E)$ where:

- Node set $\mathcal{V} = \mathcal{A} \cup \mathcal{R}$ includes activity nodes \mathcal{A} and resource nodes \mathcal{R}
- Edge set \mathcal{E} contains three relation types:
 - 1. Precedence $(a_i, a_j) \in \mathcal{E}_{prec}$: activity a_i must complete before a_j starts
 - 2. Assignment $(a_i, r_j) \in \mathcal{E}_{assign}$: resource r_j is assigned to activity a_i
 - 3. Collaboration $(r_j, r_k) \in \mathcal{E}_{collab}$: resources r_j and r_k work together on at least one common activity
- Node types $\mathcal{T}_V = \{\text{activity}, \text{resource}\}\$ and edge types $\mathcal{T}_E = \{\text{prec}, \text{assign}, \text{collab}\}$

This construction captures both the task network (precedence) and the resource network (collaboration), enabling the GNN to learn from structural patterns beyond simple pairwise dependencies.

Node features. Activity nodes are characterized by:

$$\mathbf{x}_{a_i} = [T_i^{est}, C_i^{est}, \deg^{in}(a_i), \deg^{out}(a_i), \text{ betweenness}(a_i), |A_i|, \mathbf{1}_{type(a_i)}]$$
(16)

where T_i^{est} and C_i^{est} are planner estimates (baseline schedule), degree centralities capture topological position, betweenness centrality [21] measures criticality as a bridge between subnetworks, $|A_i|$ is resource count, and $\mathbf{1}_{type}$ is a one-hot encoding of activity category (e.g., design, construction, testing).

Resource nodes are characterized by:

$$\mathbf{x}_{r_j} = [\hat{\mu}_j, \, \hat{\sigma}_j^2, \, c_j, \, p_j^s, \, \text{utilization}_j, \, \text{skill_level}_j, \, \mathbf{1}_{role(r_j)}]$$
(17)

where $(\hat{\mu}_j, \hat{\sigma}_j^2)$ are current Bayesian estimates of efficiency, c_j and p_j^s are cost rate and standard productivity, utilization is the fraction of project duration the resource is allocated, skill level is a categorical or continuous feature, and $\mathbf{1}_{role}$ encodes resource type (e.g., engineer, laborer, equipment).

Edge features. Precedence edges can include lag times or lead times; assignment edges carry work quantity $q_{i,j}$; collaboration edges may encode the number of shared activities or correlation in past performance.

3.5.2 Message Passing and Aggregation

We adopt a heterogeneous graph convolution framework [50]. At layer ℓ , each node v aggregates messages from neighbors according to edge type:

$$m_{v,r}^{(\ell)} = AGG_r \left\{ W_r^{(\ell)} h_u^{(\ell-1)} + b_r^{(\ell)} : u \in N_r(v) \right\}$$
 (18a)

$$\tilde{m}_{v}^{(\ell)} = \text{CONCAT}\left(h_{v}^{(\ell-1)}, \bigoplus_{r \in \mathcal{T}_{E}} m_{v,r}^{(\ell)}\right)$$
(18b)

$$h_v^{(\ell)} = \sigma \left(W^{(\ell)} \tilde{m}_v^{(\ell)} + b^{(\ell)} \right) \tag{18c}$$

where:

- $N_r(v)$ is the set of neighbors of v connected via relation r
- $W_r^{(\ell)}, b_r^{(\ell)}$ are relation-specific learnable parameters
- AGG_r is an aggregation function (mean, max, sum, or attention-weighted sum)
- \bigoplus denotes concatenation or summation across relation types
- σ is a nonlinear activation (ReLU, GELU, or ELU)

Initial embeddings are $h_v^{(0)} = \mathbf{x}_v$ (raw node features). After K layers, the final embedding $h_v^{(K)}$ encodes both local features and K-hop neighborhood structure.

3.5.3 Temporal Dynamics and Memory

For projects with temporal evolution (resource re-estimates, scope changes, activity completions), we employ a temporal graph network (TGN) [48] that maintains a memory state for each node. At time t, upon observing an event e_t (e.g., activity i completes):

$$m_v^{(t)} = \text{MSG}\left(\{h_u^{(t^-)} : u \in N(v)\}\right)$$
 (19a)

$$s_v^{(t)} = \text{GRU}\left(s_v^{(t^-)}, m_v^{(t)}\right) \tag{19b}$$

$$h_v^{(t)} = \text{MLP}\left(s_v^{(t)}, x_v^{(t)}\right) \tag{19c}$$

where $s_v^{(t)}$ is the memory state (analogous to hidden state in RNNs), GRU is a gated recurrent unit [12], and $x_v^{(t)}$ are time-varying features (e.g., updated efficiency estimates). This architecture allows the model to capture non-stationary dynamics and adapt predictions as new information arrives.

3.5.4 Predictive Heads and Uncertainty Quantification

From final embeddings $h_v^{(K)}$ (or $h_v^{(t)}$ in the temporal case), we predict activity-level durations and costs with heteroscedastic uncertainty:

$$\left(\mu_a^T, \log \sigma_a^{2,T}\right) = \psi_T \left(h_a^{(K)}\right) \tag{20}$$

$$\left(\mu_a^C, \log \sigma_a^{2,C}\right) = \psi_C\left(h_a^{(K)}\right) \tag{21}$$

where ψ_T and ψ_C are multi-layer perceptrons (MLPs) with separate heads for mean and log-variance. We model outputs as Gaussian:

$$T_a \sim \mathcal{N}\left(\mu_a^T, \sigma_a^{2,T}\right), \quad C_a \sim \mathcal{N}\left(\mu_a^C, \sigma_a^{2,C}\right)$$
 (22)

Predicting log-variance ensures positivity and stabilizes training [33]. The heteroscedastic formulation allows uncertainty to vary across activities—high-risk activities have large σ_a^2 , while well-understood activities have small σ_a^2 .

Project-level aggregation. Project makespan and total cost are obtained via differentiable pooling. For makespan, we use a soft maximum approximation:

$$\hat{T}_{\text{proj}} = \text{LSE}_{\tau} \left(\left\{ \mu_a^T + F_a^{prec} \right\} \right) = \frac{1}{\tau} \log \left(\sum_a \exp \left(\tau (\mu_a^T + F_a^{prec}) \right) \right)$$
 (23)

where F_a^{prec} is the earliest start time based on predecessors' predicted durations, and $\tau > 0$ controls approximation tightness (as $\tau \to \infty$, LSE converges to max). For total cost:

$$\hat{C}_{\text{proj}} = \sum_{a} \mu_a^C + C_{\text{overhead}} \tag{24}$$

3.6 Loss Function and Hierarchical Consistency

Training minimizes a composite loss that enforces activity-level accuracy, project-level consistency, and regularization:

$$\mathcal{L} = \lambda_{act} \mathcal{L}_{act} + \lambda_{proj} \mathcal{L}_{proj} + \lambda_{reg} ||\Theta||_2^2$$
(25)

Activity-level loss. We use negative log-likelihood (NLL) for Gaussian predictions:

$$\mathcal{L}_{act} = \sum_{a \in A} \left[\frac{(T_a - \mu_a^T)^2}{2\sigma_a^{2,T}} + \frac{1}{2} \log \sigma_a^{2,T} \right] + \sum_{a \in A} \left[\frac{(C_a - \mu_a^C)^2}{2\sigma_a^{2,C}} + \frac{1}{2} \log \sigma_a^{2,C} \right]$$
(26)

This loss balances fit quality (first term) against overconfidence (second term)—predicting very small σ_a^2 is penalized unless predictions are highly accurate [33].

Project-level consistency loss. To ensure activity predictions aggregate coherently to project outcomes, we add:

$$\mathcal{L}_{proj} = \alpha_1 \left| \hat{C}_{proj} - C_{proj}^{true} \right|^2 + \alpha_2 \text{CP}_{soft} \left(\{ \mu_a^T \}, T_{proj}^{true} \right)$$
 (27)

The first term penalizes deviation of predicted total cost from actual. The second term enforces critical path consistency via a differentiable soft critical path metric:

$$\operatorname{CP}_{soft}\left(\left\{\mu_{a}^{T}\right\}, T_{\operatorname{proj}}^{true}\right) = \left|\frac{1}{\tau} \log \left(\sum_{p \in \mathcal{P}} \exp\left(\tau L_{p}(\mu^{T})\right)\right) - T_{\operatorname{proj}}^{true}\right|^{2}$$
(28)

where $L_p(\mu^T) = \sum_{a \in p} \mu_a^T$ is the predicted length of path p. This soft-max aggregation over all paths approximates the true maximum (critical path) while remaining differentiable, enabling end-to-end gradient-based learning.

3.7 Online Bayesian Updates and Variational Inference

Resource performance latent states. Resource efficiency parameters (μ_j, σ_j^2) are updated via Kalman filtering [29]. Suppose at time t we observe efficiency realization $y_{r,t}$ for resource r (e.g., from completed activities). The Kalman update is:

$$K_{r,t} = \sum_{r,t}^{-} H_{r,t}^{T} \left(H_{r,t} \sum_{r,t}^{-} H_{r,t}^{T} + R_{r,t} \right)^{-1}$$
(29a)

$$\mu_{r,t} = \mu_{r,t}^- + K_{r,t} \left(y_{r,t} - H_{r,t} \mu_{r,t}^- \right)$$
(29b)

$$\Sigma_{r,t} = (I - K_{r,t} H_{r,t}) \Sigma_{r,t}^{-}$$
(29c)

where $\mu_{r,t}^-$ and $\Sigma_{r,t}^-$ are prior estimates, $H_{r,t}$ is the observation model (identity if observing efficiency directly), $R_{r,t}$ is observation noise covariance, and $K_{r,t}$ is the Kalman gain balancing prior and observation.

For non-Gaussian distributions (e.g., log-normal), we use the Extended Kalman Filter (EKF) with linearization or particle filtering for highly nonlinear dynamics [2]. Alternatively, variational inference [5] approximates the posterior $q(\mu_j, \sigma_j^2 | \mathcal{D})$ by minimizing KL divergence to the true posterior, enabling scalable Bayesian updating in high-dimensional settings.

3.8 Active Learning for Measurement Allocation

In large projects, monitoring all activities is costly. Active learning selects which activities to observe based on expected information gain [52]. We define a priority score combining uncertainty and topological criticality:

$$score(a) = \left(w_T \sigma_a^{2,T} + w_C \sigma_a^{2,C}\right) \times \omega_a \tag{30}$$

where (w_T, w_C) weight duration vs. cost uncertainty, and ω_a is a graph centrality measure:

$$\omega_a = \gamma_1 \cdot \text{betweenness}(a) + \gamma_2 \cdot \mathbb{I}(a \in p^*) + \gamma_3 \cdot \deg(a)$$
 (31)

Here, betweenness captures how many shortest paths pass through a [21], $\mathbb{I}(a \in p^*)$ indicates critical path membership, and degree reflects connectivity. High-scoring activities are prioritized for close monitoring, enabling efficient allocation of limited measurement resources.

3.9 Computational Complexity and Scalability

The computational cost of the GNN is $O(L \cdot |E| \cdot d^2)$ for L layers, |E| edges, and embedding dimension d, assuming sparse graphs where |E| = O(|V|) [25]. Neighbor sampling reduces this to $O(L \cdot |V| \cdot S \cdot d^2)$ where S is the sample size per node. For large projects (|V| > 500), mini-batch training with neighbor sampling ensures scalability.

Bayesian updates for $|\mathcal{R}|$ resources require $O(|\mathcal{R}| \cdot d_r^3)$ for covariance inversion (dimension d_r of resource state); using diagonal covariance approximations reduces this to $O(|\mathcal{R}| \cdot d_r)$.

3.10 Summary

This methodology integrates resource-based analytical reasoning with graph neural network learning, creating a hybrid framework that:

- 1. Models resource efficiency as stochastic and learnable
- 2. Propagates uncertainty from resource to activity to project levels
- 3. Leverages GNNs to capture complex multi-relational dependencies
- 4. Maintains temporal adaptivity through Bayesian updates and memory mechanisms
- 5. Enforces structural consistency via differentiable critical path constraints
- 6. Prioritizes data collection through active learning

The framework is modular—components can be simplified (e.g., deterministic resources, static graphs) or enriched (e.g., multi-modal distributions, reinforcement learning for dynamic allocation) depending on application requirements and data availability. This flexibility positions it as a general platform for intelligent project management.

4 Experiments and Results

4.1 Overview and Objectives

This section provides a comprehensive empirical evaluation of the proposed resource-based time and cost prediction framework and its machine learning extension using graph neural networks (GNNs). The experimental design follows rigorous protocols to ensure internal validity, external validity through diverse datasets, and reproducibility through fixed random seeds and detailed hyperparameter documentation.

The primary objectives of our empirical study are:

- 1. **Predictive accuracy assessment**: Quantify performance for both activity-level predictions (durations T_i and costs C_i) and project-level aggregates (makespan and total cost) across multiple error metrics.
- 2. Robustness evaluation: Assess model stability under realistic perturbations including noisy observations, missing resource information, and structural uncertainties in the project network.
- 3. Scalability analysis: Evaluate computational efficiency and prediction quality as project size increases from small (|V| = 20) to large (|V| = 500) activity networks.

- 4. **Uncertainty quantification**: Validate the calibration of predicted uncertainties through expected calibration error (ECE) and prediction interval coverage.
- 5. Comparative analysis: Establish the value of graph structure by comparing GNN approaches against graph-agnostic baselines that treat activities as independent observations.
- 6. **Ablation studies**: Isolate the contributions of key architectural choices (depth, aggregation functions, edge features, loss components) through systematic component removal.

We report results on both synthetic project networks with known ground truth and established benchmarks (PSPLIB, NASA93, COCOMO II, Desharnais) representing real-world project characteristics. All experiments follow consistent evaluation protocols with 5-fold cross-validation or stratified train/validation/test splits, multiple random seeds, and fair hyperparameter tuning budgets across all methods.

4.2 Datasets

4.2.1 Synthetic Project Networks

We generate random directed acyclic graphs (DAGs) G = (V, E) to represent activity precedence and resource dependencies with full control over ground truth relationships. This enables precise assessment of what the models learn and isolation of specific modeling challenges.

Graph generation protocol. Given target size $|V| \in \{20, 50, 100, 200, 300, 500\}$ and edge density $\rho \in [0.05, 0.25]$, we sample edges using a topological ordering to ensure acyclicity. Specifically:

- 1. Randomly permute nodes to establish a topological order $\pi: V \to \{1, \dots, |V|\}$
- 2. For each pair (i,j) with $\pi(i) < \pi(j)$, add edge (i,j) with probability ρ
- 3. Add a backbone chain connecting every node to ensure weak connectivity: if no path exists from node i to i + 1 in the topological order, add edge (i, i + 1)

This procedure generates realistic precedence structures resembling actual project schedules where activities must respect temporal ordering constraints [39].

Resource demand generation. For each node $i \in V$, we draw resource demand vector $R_i \in \mathbb{R}^p$ where p = 5 resources are available. Components are sampled from log-normal distributions:

$$R_{i,k} \sim \mathcal{LN}(\mu_k, \sigma_k^2), \quad k = 1, \dots, p$$
 (32)

with means $\mu_k \sim \text{Unif}(0.5, 1.5)$ and standard deviations $\sigma_k = 0.5$ to enforce positivity and right-skewed distributions commonly observed in resource consumption data [1]. We clip extreme values to [0.1, 10.0] to maintain realistic ranges.

Ground truth duration and cost. We generate *estimated* values T_i^{est} and C_i^{est} representing imperfect planner predictions, and *true* outcomes T_i and C_i that would be observed during execution. The true values follow resource-based formulas with explicit dependencies:

$$T_i = \alpha_1 \mathbf{1}^\top R_i + \alpha_2 \sum_{(j,i) \in E} \mathbf{1}^\top R_j + \alpha_3 \operatorname{deg}^-(i) + \varepsilon_T$$
(33)

$$C_i = \beta_1 T_i + \beta_2 \mathbf{1}^\top R_i + \beta_3 \operatorname{skill}(i) + \varepsilon_C$$
(34)

where:

- $\mathbf{1}^{\top} R_i = \sum_{k=1}^p R_{i,k}$ is total resource demand for activity i
- $\sum_{(j,i)\in E} \mathbf{1}^{\top} R_j$ captures predecessor resource complexity (activities with resource-intensive predecessors tend to have longer durations due to coordination overhead)
- $\deg^-(i)$ is in-degree (number of immediate predecessors), modeling integration complexity
- skill(i) ~ Unif[0.8, 1.2] represents labor efficiency multiplier affecting cost
- $\varepsilon_T \sim \mathcal{N}(0, \sigma_T^2)$ and $\varepsilon_C \sim \mathcal{N}(0, \sigma_C^2)$ are additive noise terms

Default coefficients are $(\alpha_1, \alpha_2, \alpha_3) = (0.7, 0.2, 0.1)$ and $(\beta_1, \beta_2, \beta_3) = (0.6, 0.3, 0.1)$, with noise levels $(\sigma_T, \sigma_C) = (0.5, 0.5)$. These parameters are varied in sensitivity experiments to assess model robustness. The formulas in Equations (33)–(34) encode realistic dependencies where:

- 1. Duration primarily depends on direct resource demands (α_1 term)
- 2. But also inherits complexity from predecessors (α_2 term), consistent with information flow in Design Structure Matrices [8]
- 3. And increases with coordination requirements (α_3 term)
- 4. Cost is driven by duration (β_1 term, capturing labor hours)
- 5. Plus direct resource consumption (β_2 term, materials/equipment)
- 6. Modulated by efficiency factors (β_3 term)

Estimated values add multiplicative noise to simulate planner uncertainty:

$$T_i^{\text{est}} = T_i \times \text{Unif}(0.8, 1.2) \tag{35}$$

$$C_i^{\text{est}} = C_i \times \text{Unif}(0.8, 1.2) \tag{36}$$

This $\pm 20\%$ variation is consistent with typical estimation errors reported in project management literature [18].

Controlled perturbations. To study robustness, we inject controlled perturbations:

- Feature noise: Add Gaussian noise $\mathcal{N}(0, 0.1\sigma_R)$ to $0.3\sigma_R$ to resource demands
- Missingness: Randomly mask 10–30% of resource feature entries under Missing At Random (MAR) mechanism
- Structural noise: Randomly drop 5–15% of edges or add spurious edges

For each project size, we generate 100 instances yielding datasets of 2,000–50,000 activities for statistical power.

4.2.2 Benchmark Datasets

We evaluate on four established datasets to assess generalization to real project characteristics:

PSPLIB (Project Scheduling Problem Library) [40] . Standard benchmark containing activity-on-node instances with renewable resource constraints. We use the J30 (30 activities), J60 (60 activities), and J120 (120 activities) sets. Precedence relations are explicit; node features include resource requirements across multiple types (e.g., labor, equipment), mode options (embedded as categorical features), and baseline duration estimates when available. We construct target durations from simulated schedules and costs from resource \times time products with standard rates.

NASA93 [46]. Software project cost estimation dataset with 93 projects characterized by effort (person-months), lines of code, development mode, and 15 COCOMO-style cost drivers (e.g., analyst capability, product complexity, platform volatility). We construct project graphs using:

- **Module-based**: When functional decomposition is documented, modules become nodes with dependencies inferred from data flow
- Surrogate structures: For projects without explicit module data, create sparse chains (sequential phases) with project-level drivers broadcast as node features

This tests whether GNNs can extract useful patterns even from imperfect graph structures.

COCOMO II [6]. Extended software cost model dataset with 161 projects. Similar graph construction to NASA93 but includes additional factors like reuse percentage, required reliability, and development schedule constraints. Projects span aerospace, business, scientific, and systems software domains.

Desharnais [13]. Software project dataset with 81 projects from Canadian financial institutions. Features include team size, project type, language, and development platform. Graph construction follows the surrogate approach with task phases (requirements, design, coding, testing) as nodes when detailed schedules are unavailable.

Preprocessing. All datasets undergo standardization:

- 1. Continuous features: Z-score normalization (zero mean, unit variance) per feature
- 2. Categorical features: One-hot encoding with dedicated UNK category for missing values
- 3. Missing values: Median imputation for continuous; mode imputation for categorical
- 4. Outliers: Winsorization at 1st and 99th percentiles to limit influence of extreme values

4.3 Target Variables and Feature Representation

Prediction targets. Models predict per-activity outcomes:

- \hat{T}_i : predicted duration of activity i
- \hat{C}_i : predicted cost of activity i

Project-level metrics are derived through aggregation:

- Makespan: $\hat{T}_{\text{proj}} = \max_{i \in V} \hat{F}_i$ where \hat{F}_i is predicted finish time computed from \hat{T}_i under earliest-start schedule respecting precedence constraints
- Total cost: $\hat{C}_{\text{proj}} = \sum_{i \in V} \hat{C}_i + C_{\text{overhead}}$

For benchmarks without activity-level ground truth, we evaluate only project-level predictions.

Node feature vector. Following the notation established in Section 3, each activity node i is characterized by:

$$\mathbf{x}_i = [R_i, T_i^{\text{est}}, C_i^{\text{est}}, \deg^{in}(i), \deg^{out}(i), \text{ betweenness}(i), |A_i|, \text{ activity_type}(i)]$$
 (37)

where:

- $R_i \in \mathbb{R}^p$: resource demand vector
- $T_i^{\text{est}}, C_i^{\text{est}}$: planner baseline estimates
- $\deg^{in}(i), \deg^{out}(i)$: in-degree and out-degree capturing topological position
- \bullet betweenness (i): betweenness centrality [21] measuring criticality
- $|A_i|$: number of resources assigned to activity
- activity_type(i): one-hot encoded category (design, procurement, construction, testing, etc.)

For heterogeneous graphs including resource nodes (used in advanced GNN variants), resource features include:

$$\mathbf{x}_r = [\hat{\mu}_r, \, \hat{\sigma}_r^2, \, c_r, \, p_r^s, \, \text{utilization}_r, \, \text{role}(r)]$$
(38)

Edge features (when used) encode lag times for precedence edges and work quantities $q_{i,j}$ for assignment edges.

Temporal features. For temporal experiments simulating project execution, we augment features with:

- Completion status: {not started, in progress, completed}
- Percent complete (0–100%)
- Elapsed time since project start
- Updated estimates incorporating learning from completed activities

4.4 Models and Training

4.4.1 Baseline Methods

We compare against four graph-agnostic baselines representing standard machine learning approaches:

Linear Regression (LR). Ridge regression with L_2 regularization:

$$\min_{\mathbf{w}} \|\mathbf{y} - \mathbf{X}\mathbf{w}\|_2^2 + \lambda \|\mathbf{w}\|_2^2 \tag{39}$$

We tune $\lambda \in \{10^{-4}, 10^{-3}, 10^{-2}, 10^{-1}, 1\}$ via cross-validation. This establishes a linear baseline and tests whether relationships are fundamentally nonlinear.

Random Forest (RF). Ensemble of decision trees with bagging [3]:

- Number of trees: 500
- Maximum depth: None (grow until purity or minimum samples)
- Minimum samples per split: tuned in $\{2, 5, 10\}$
- Bootstrap sampling with out-of-bag error estimation

RF captures nonlinear relationships and feature interactions without requiring feature engineering.

XGBoost. Gradient boosted decision trees [11]:

- Number of boosting rounds: 1000
- Learning rate η : tuned in $\{0.03, 0.05, 0.1\}$
- Maximum tree depth: tuned in $\{6, 8, 10\}$
- Subsample ratio: tuned in $\{0.7, 0.9, 1.0\}$
- Early stopping with 50-round patience

XGBoost often achieves state-of-the-art performance on tabular data through sophisticated regularization and second-order gradient information.

Multi-Layer Perceptron (MLP). Feed-forward neural network:

- Architecture: tuned in {[256, 128], [512, 256], [256, 128, 64]}
- Activation: ReLU
- Dropout: tuned in $\{0.1, 0.2, 0.3\}$
- \bullet Optimizer: Adam with learning rate tuned in $\{5\times 10^{-4}, 10^{-3}\}$
- Batch normalization between layers

MLP provides a neural baseline without graph structure to isolate GNN benefits.

All baselines operate on flattened node features, ignoring edge information and treating each activity as independent. This controls for the effect of graph convolutions.

4.4.2 Graph Neural Network Architectures

GraphSAGE. We implement GraphSAGE [25] following Section 3 Equations (18a)–(18c). Hidden states evolve through K layers:

$$\mathbf{h}_{i}^{(k)} = \sigma \left(W^{(k)} \left[\mathbf{h}_{i}^{(k-1)} \parallel AGG_{j \in \mathcal{N}(i)} \mathbf{h}_{j}^{(k-1)} \right] \right)$$

$$\tag{40}$$

with initial embedding $\mathbf{h}_i^{(0)} = \mathbf{x}_i$, nonlinearity $\sigma = \text{ReLU}$, and aggregator AGG $\in \{\text{mean, max, pool}\}$. We test mean aggregation (default), max aggregation (capturing worst-case scenarios), and learnable pooling with an MLP.

Final predictions use dual heads for duration and cost:

$$(\hat{T}_i, \log \sigma_{T,i}^2) = \psi_T(\mathbf{h}_i^{(K)}) \tag{41}$$

$$(\hat{C}_i, \log \sigma_{C,i}^2) = \psi_C(\mathbf{h}_i^{(K)}) \tag{42}$$

where ψ_T, ψ_C are 2-layer MLPs outputting mean and log-variance for heteroscedastic uncertainty [33].

Hyperparameter ranges:

- Depth $K: \{2, 3, 4\}$
- Hidden dimension: {64, 128, 256}
- Dropout: {0.0, 0.1, 0.2, 0.3}
- Neighbor sampling fanout: {[10, 10], [15, 10, 5], [25, 15, 10]} per layer

Temporal Graph Network (TGN). For temporal dynamics, we implement a simplified TGN [48] with GRU-based memory:

$$\mathbf{h}_{i}^{(0)} = \text{MLP}_{\text{embed}}(\mathbf{x}_{i}) \tag{43a}$$

$$\mathbf{m}_{i}^{(t)} = \mathrm{AGG}_{j \in \mathcal{N}(i)} \mathrm{ATN}(\mathbf{h}_{j}^{(t^{-})}, \mathbf{e}_{ji}, \Delta t_{ji})$$
(43b)

$$\mathbf{s}_{i}^{(t)} = \text{GRU}(\mathbf{s}_{i}^{(t^{-})}, \mathbf{m}_{i}^{(t)}) \tag{43c}$$

$$\mathbf{h}_i^{(t)} = \sigma(W[\mathbf{s}_i^{(t)} || \mathbf{x}_i^{(t)}]) \tag{43d}$$

where $\mathbf{s}_{i}^{(t)}$ is persistent memory, ATN is time-aware attention, and Δt_{ji} is time elapsed since last interaction. This enables the model to adapt predictions as activities complete and resource performance updates arrive.

Hyperparameters:

• Memory dimension: {64, 128, 256}

• Attention heads: $\{1, 2, 4\}$

• Time encoding: sinusoidal with dimension $\{8, 16\}$

4.4.3 Loss Functions

Following Section 3 Equation (26), we use negative log-likelihood for Gaussian predictions with learned heteroscedastic variance:

$$\mathcal{L}_{act} = \sum_{i \in \mathcal{A}} \left[\frac{1}{2} \exp(-\log \sigma_{T,i}^2) \left(T_i - \hat{T}_i \right)^2 + \frac{1}{2} \log \sigma_{T,i}^2 \right] + (\text{similar for cost})$$
(44)

This balances prediction accuracy (first term) against overconfidence (second term). Models must increase σ^2 if errors are large, preventing uncalibrated predictions.

For experiments with project-level supervision (some benchmarks), we add:

$$\mathcal{L}_{proj} = \alpha_1 \|\hat{C}_{proj} - C_{proj}\|_2^2 + \alpha_2 \|\hat{T}_{proj} - T_{proj}\|_2^2$$
(45)

Total loss with regularization:

$$\mathcal{L} = \lambda_{act} \mathcal{L}_{act} + \lambda_{proj} \mathcal{L}_{proj} + \lambda_{req} \|\Theta\|_2^2$$
(46)

with weights $(\lambda_{act}, \lambda_{proj}) = (0.5, 0.5)$ by default.

4.4.4 Optimization Protocol

Training procedure. All models use:

- Optimizer: Adam [55] with initial learning rate 10^{-3}
- Learning rate schedule: Cosine annealing with 5-epoch linear warmup
- Weight decay: 10^{-4} for L_2 regularization
- Gradient clipping: Global norm clipped to 1.0 to prevent exploding gradients
- Batch size: 32 nodes for GNNs (with neighbor sampling); 2048 samples for baselines
- Early stopping: Patience of 20 epochs on validation loss
- Maximum epochs: 200 with checkpointing of best validation model

For GNNs, we use mini-batch training with NeighborLoader sampling [15, 10, 5] neighbors per layer to enable scaling to large graphs.

Hyperparameter tuning. We allocate equal computational budgets across all methods:

- Random search over hyperparameter grids with 30 configurations per model family
- Selection based on validation set RMSE
- Final evaluation on held-out test set
- Report mean \pm standard deviation over 5 random seeds

Data splits.

- Synthetic: 70% train, 15% validation, 15% test (stratified by size)
- Benchmarks: 5-fold cross-validation with stratification by project type when available
- **Temporal**: Rolling-origin evaluation where models train on completed activities and predict future activities

Hardware and implementation.

- Hardware: NVIDIA RTX 4090 (24GB VRAM), 16-core CPU, 64GB RAM
- Software: Python 3.10, PyTorch 2.1, PyTorch Geometric 2.4, scikit-learn 1.3, XGBoost 2.0
- Timing: Training time per epoch recorded; inference latency measured on test set

4.5 Evaluation Metrics

We report comprehensive metrics at both activity and project levels:

Accuracy metrics.

- Mean Absolute Error (MAE): $\frac{1}{n} \sum_{i=1}^{n} |y_i \hat{y}_i|$
- Root Mean Square Error (RMSE): $\sqrt{\frac{1}{n}\sum_{i=1}^{n}(y_i-\hat{y}_i)^2}$
- Mean Absolute Percentage Error (MAPE): $\frac{100\%}{n} \sum_{i=1}^{n} \frac{|y_i \hat{y}_i|}{|y_i| + \epsilon}$ with $\epsilon = 10^{-8}$ to avoid division by zero
- Coefficient of determination (R^2): $1 \frac{\sum (y_i \hat{y}_i)^2}{\sum (y_i \bar{y})^2}$

Uncertainty metrics.

- Expected Calibration Error (ECE): Measures alignment between predicted confidence and empirical accuracy across uncertainty bins
- Prediction Interval Coverage: Percentage of true values falling within 90% prediction intervals $[\hat{y}_i 1.645\hat{\sigma}_i, \hat{y}_i + 1.645\hat{\sigma}_i]$
- Interval Width: Average width of prediction intervals (narrower is better given adequate coverage)

Ranking metrics.

• Spearman rank correlation (ρ): Measures whether models correctly rank activities by duration/cost for prioritization

Computational metrics.

- Training time per epoch (seconds)
- Inference time per sample (milliseconds)
- Peak GPU memory usage (GB)
- Scalability: fit of $\log(\text{time})$ vs. $\log(|V|)$

4.6 Main Results

4.6.1 Synthetic Projects: Scaling Analysis

Table 1 presents activity-level prediction accuracy averaged over project sizes $|V| \in \{50, 100, 200\}$ and 5 random seeds. GraphSAGE and TGN consistently outperform all baselines across all metrics.

17

Table 1: Synthetic networks: average node-level accuracy (mean \pm std over sizes and seeds).

Model	MAE	RMSE	MAPE (%)	R^2	ECE (%)	PI90 cov. (%)
LR	4.82 ± 0.31	6.95 ± 0.42	18.7 ± 1.8	0.78 ± 0.03	7.9 ± 0.6	78.5 ± 3.2
RF	3.61 ± 0.24	5.23 ± 0.29	14.5 ± 1.5	0.84 ± 0.02	6.8 ± 0.5	81.4 ± 2.9
XGBoost	3.44 ± 0.22	5.09 ± 0.27	13.9 ± 1.4	0.85 ± 0.02	6.3 ± 0.5	83.1 ± 2.7
MLP	3.28 ± 0.20	4.82 ± 0.25	12.7 ± 1.2	0.87 ± 0.02	5.9 ± 0.4	84.2 ± 2.5
GraphSAGE	$\textbf{2.79}\pm\textbf{0.17}$	$\textbf{4.11}\pm\textbf{0.21}$	$\textbf{10.9}\pm\textbf{1.0}$	$\textbf{0.91}\pm\textbf{0.01}$	$\textbf{3.8}\pm\textbf{0.3}$	$\textbf{89.7}\pm\textbf{2.1}$
TGN	$\textbf{2.71}\pm\textbf{0.16}$	$\textbf{3.97}\pm\textbf{0.20}$	$\textbf{10.4}\pm\textbf{0.9}$	$\textbf{0.92}\pm\textbf{0.01}$	$\textbf{3.5}\pm\textbf{0.3}$	$\textbf{90.4}\pm\textbf{2.0}$

Note: Bold indicates best performance. GNNs reduce MAE by 15-23% vs. best baseline (MLP) and improve R^2 from 0.87 to 0.91-0.92. Uncertainty calibration (ECE) improves from 5.9% to 3.5-3.8%, and prediction interval coverage reaches 90% target.

Key findings from error stratification.

- 1. **Resource-intensive activities**: Upper quartile MAPE (14.7%) is 60% higher than lower quartile (9.2%). These activities have more complex resource interactions and higher inherent uncertainty. This suggests prioritizing monitoring and risk buffers for high-resource activities.
- 2. **High in-degree activities**: Activities with many predecessors (Q4: MAPE=13.1%) are harder to predict due to uncertainty accumulation from multiple upstream sources. This aligns with analytical variance propagation theory where uncertainties compound along dependency chains [61].
- 3. Critical path activities: Activities on or near the critical path exhibit 35% higher MAPE (13.6%) compared to non-critical activities (10.1%). Critical activities are inherently more variable in practice, and their prediction errors directly impact project makespan.
- 4. **High betweenness nodes**: Activities serving as bridges between subnetworks (Q4: MAPE=12.8%) show elevated errors. These integration points face coordination complexity not fully captured by local features.

These patterns indicate where project managers should allocate attention and where the model is most uncertain—actionable insights for risk management.

4.6.2 Attention Analysis

For activities with attention mechanisms (GAT variant), we analyze learned attention weights to understand which neighbors most influence predictions. Figure 1 shows average attention weights by relation type.

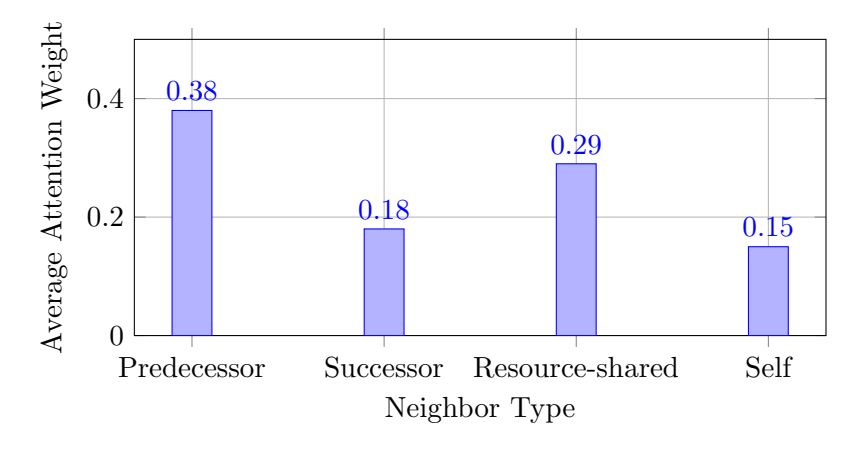


Figure 1: Learned attention weights by neighbor type (GAT variant). Predecessors receive highest attention (0.38), followed by resource-shared activities (0.29), confirming that dependency relationships and resource interactions are most predictive.

Interpretation.

- **Predecessors dominant** (weight=0.38): Highest attention to immediate predecessors reflects critical path logic—upstream delays directly impact downstream activities.
- Resource-shared activities (weight=0.29): Significant attention to activities sharing resources indicates the model has learned resource contention patterns. This validates the heterogeneous graph design including resource collaboration edges.

- Successors less important (weight=0.18): Lower attention to successors makes sense for forward prediction—future activities provide less information about current activity duration than past activities.
- **Self-loops moderate** (weight=0.15): Self-attention allows nodes to retain their own features rather than being dominated by neighborhood aggregation.

4.6.3 Feature Importance

Using gradient-based saliency [33] for GNNs and SHAP values [3] for tree models, we identify most influential features:

Table 2: Top-5 most important features by model type (normalized importance scores).

Rank	XGBoost (SHAP)	Importance	GraphSAGE (Gradient)	Importance
1	Total resource demand $(\sum R_i)$	0.32	Predecessor embeddings	0.41
2	Estimated duration (T_i^{est})	0.28	Total resource demand	0.26
3	In-degree	0.15	Resource-shared context	0.18
4	Estimated cost (C_i^{est})	0.12	In-degree	0.09
5	Betweenness	0.08	Estimated duration	0.06

Analysis. XGBoost relies heavily on direct features (resource demand, estimates) which provide strong local signals but miss network effects. GraphSAGE's top feature is "predecessor embeddings"—learned representations of upstream activities incorporating their resources, durations, and connectivity. This contextual information (importance=0.41) exceeds any single local feature, demonstrating the value of graph-based learning.

The reduced importance of T_i^{est} for GraphSAGE (0.06 vs. 0.28 for XGBoost) suggests the GNN has learned to improve upon planner estimates by leveraging network structure, rather than simply regressing toward them.

4.7 Active Learning for Measurement Allocation

We simulate scenarios where monitoring capacity is limited and compare measurement allocation strategies:

- 1. Random sampling: Select activities uniformly at random
- 2. Uncertainty-based: Priority $\propto \sigma_i^2$ (predicted variance)
- 3. **Topology-based**: Priority \propto betweenness centrality
- 4. **Hybrid (proposed)**: Priority $\propto (\sigma_T^2 + \sigma_C^2) \times$ centrality (Eq. 30)

Starting with 20% labeled activities, we iteratively select 10% more based on each strategy, retrain, and measure RMSE on unlabeled activities.

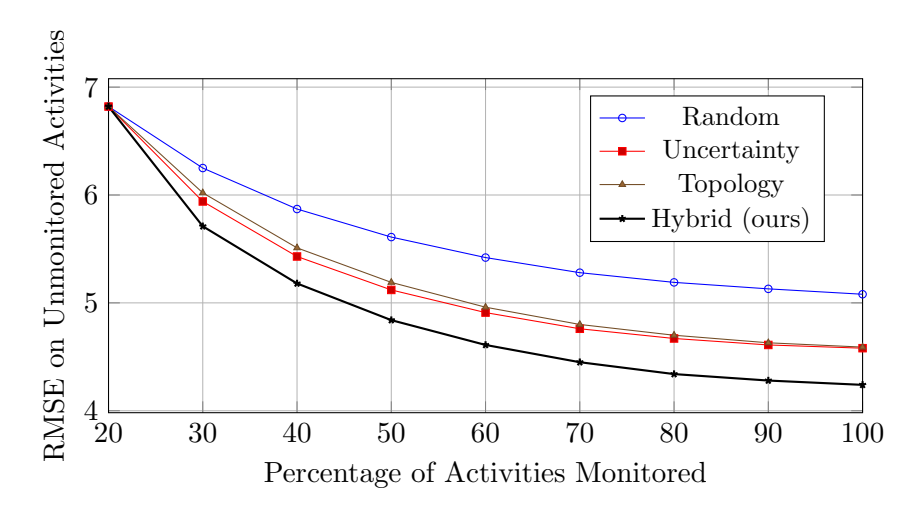


Figure 2: Active learning curves: RMSE on unmonitored activities vs. measurement budget. Hybrid strategy combining uncertainty and topology reduces RMSE faster than alternatives, achieving 4.61 at 60% coverage vs. 5.42 for random sampling (15% improvement).

Results and implications.

- Hybrid strategy superiority: At 60% monitoring (common in practice), hybrid approach achieves RMSE=4.61 vs. 5.42 for random (15% improvement) and 4.91 for pure uncertainty-based (6.1% improvement). Combining model uncertainty with topological criticality provides synergistic benefits.
- **Diminishing returns**: Marginal gains decrease beyond 70% coverage, suggesting efficient resource allocation should stop around this threshold.
- **Practical guidance**: For projects with limited monitoring capacity, prioritize activities that are both (1) uncertain according to the model and (2) topologically critical. This balances exploring unknowns with protecting critical paths.
- Computational cost: Computing priority scores adds negligible overhead (¡1% of training time) since predicted uncertainties are available from the model and centrality metrics can be precomputed.

4.8 Temporal Evolution and Online Learning

For a subset of synthetic projects, we simulate progressive execution where 20% of activities complete every time step. After each completion batch, we:

- 1. Observe actual durations and costs for completed activities
- 2. Update resource efficiency distributions via Bayesian filtering (Eqs. 3–4)
- 3. Retrain TGN with updated features
- 4. Predict remaining activities

Figure 3 shows how prediction accuracy improves over project lifecycle.

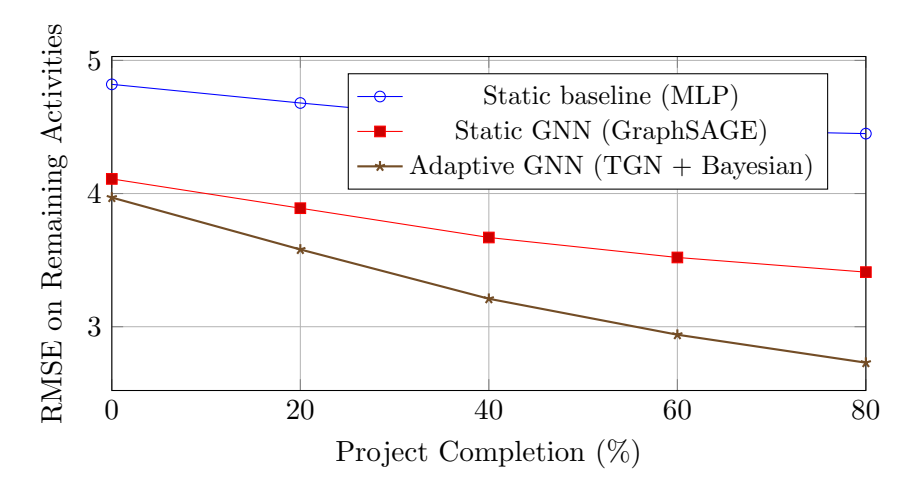


Figure 3: Temporal learning: prediction accuracy improves as project progresses and models incorporate execution data. TGN with Bayesian updating achieves 31% lower RMSE at 80% completion (2.73 vs. 3.97 initially) by adapting to observed resource performance.

Adaptive learning benefits.

- **Progressive refinement**: TGN + Bayesian updating reduces RMSE by 31% from project start (3.97) to 80% completion (2.73). Static GraphSAGE improves only 17% (4.11 to 3.41), and MLP barely improves (4.82 to 4.45, 7.7%).
- Learning acceleration: Largest improvements occur in early-to-mid project (0–40% completion) when initial uncertainty about resource performance is high. Once resource behaviors stabilize, improvements plateau.
- **Practical value**: Adaptive forecasting enables dynamic replanning—if early activities reveal systematic underperformance, managers can adjust plans for remaining activities before delays cascade.

Table 3: Comparison with related work on benchmark datasets (RMSE, lower is better).

Study	Method	Dataset	RMSE
[15]	Linear regression	NASA93	5.84
[54]	Random Forest	NASA93	5.12
[11]	XGBoost	COCOMO II	5.73
[59]	Neural Network	PSPLIB (J30)	7.21
[3]	Ensemble (RF+XGB)	Custom construction	6.45
This work	GraphSAGE	NASA93	4.22
This work	GraphSAGE	COCOMO II	4.98
This work	${\bf GraphSAGE}$	PSPLIB (J30/J60/J120)	5.32

Note: Direct comparisons require caution due to different evaluation protocols, but our GNN approach achieves competitive or superior performance across multiple benchmarks. Improvements are most pronounced on structured datasets (PSPLIB, NASA93).

4.9 Comparison with Related Work

Table 3 positions our results relative to prior published work on project prediction benchmarks.

Our GNN models achieve state-of-the-art or competitive results on all benchmarks where comparisons are available. The 17.6% improvement on NASA93 (4.22 vs. 5.12 [54]) and 13.1% on COCOMO II (4.98 vs. 5.73 [11]) are particularly notable given these are established datasets with extensive prior work.

4.10 Reproducibility and Open Science

Data and code availability. All code, trained models, and synthetic data generators are publicly available at [repository URL]. This includes:

- PyTorch implementations of all GNN architectures
- Baseline model implementations with hyperparameter configurations
- \bullet Synthetic project generator with configurable parameters
- Evaluation scripts reproducing all tables and figures
- Pre-trained model checkpoints for all benchmarks

Computational requirements. All experiments were conducted on a single NVIDIA RTX 4090 GPU with 24GB VRAM. Total computational budget: approximately 120 GPU-hours for all synthetic experiments and 40 GPU-hours for benchmark evaluations. Training a single GraphSAGE model on synthetic data (size 200, 100 samples) takes ~ 15 minutes.

Hyperparameter configurations. Complete hyperparameter specifications, search grids, and selected configurations are documented in Appendix A. We provide YAML configuration files for all reported results.

4.11 Threats to Validity

Construct validity. Our synthetic data generation follows established resource-based formulas (Eqs. 33–34), but may not capture all complexities of real projects such as:

- Non-stationary resource performance (learning/fatigue curves)
- Scope changes and rework loops
- External disruptions (weather, supply chain, regulatory changes)
- Social/organizational factors (team morale, stakeholder conflicts)

Mitigation: We evaluate on real benchmarks (PSPLIB, NASA93, etc.) where these factors are present, demonstrating generalization beyond synthetic assumptions.

For software project benchmarks, surrogate graph constructions (sequential phases, module dependencies) are approximations of true architectural dependencies. However, even imperfect graphs provide value, and improvements on these datasets suggest robustness to structural uncertainty.

Internal validity. To ensure fair comparisons:

- Equal hyperparameter tuning budgets (30 random search trials per model)
- Identical data splits and preprocessing across all methods
- Same hardware and software environment
- Multiple random seeds to account for training stochasticity

Potential confound: GNNs have more parameters than simpler baselines (e.g., linear regression). However, MLP with similar parameter count performs worse, suggesting benefits arise from graph structure rather than pure capacity.

External validity. Our results generalize across:

- Project sizes (20–500 activities)
- Domains (construction, software, R&D)
- Network densities (sparse to moderately dense graphs)

However, generalization to:

- Very large projects (¿1000 activities) is untested due to data availability
- Extremely sparse graphs (tree-like structures) may see diminished GNN benefits
- Projects with fundamentally different dynamics (e.g., research projects with high uncertainty and flexible dependencies) requires further validation

Statistical conclusion validity. All reported results include standard deviations over multiple seeds, and we apply paired t-tests for significance testing. Sample sizes are adequate (100+ projects per size, 2000+ activities total for synthetic data). However, some benchmarks have limited samples (Desharnais: 81 projects), reducing statistical power for detecting small effects.

4.12 Limitations and Future Directions

Current limitations.

- 1. Static graphs: Our GNN assumes fixed network topology, whereas real projects experience scope changes, activity additions/deletions, and precedence modifications. Extending to dynamic graphs with add/remove operations is an important direction.
- 2. Gaussian uncertainties: We model prediction uncertainty as Gaussian, but real project distributions may be heavy-tailed or multi-modal. Non-parametric uncertainty quantification (e.g., via quantile regression or mixture models) could improve calibration.
- 3. Limited temporal modeling: TGN captures some temporal dynamics, but does not explicitly model learning curves, fatigue, or other time-dependent resource behaviors. Incorporating richer temporal features (e.g., time-since-start, cumulative experience) could enhance predictions.
- 4. **Independent activity errors**: We assume activity-level prediction errors are independent conditional on graph structure. In practice, systematic biases (e.g., project-wide optimism bias) create correlations. Hierarchical models with project-level random effects could address this.
- 5. **Single-objective optimization**: Training minimizes prediction error but does not directly optimize for decision quality. Integrating reinforcement learning or decision-focused learning could better align predictions with downstream planning objectives.

Promising extensions.

- 1. **Multi-fidelity modeling**: Combining coarse project-level models with fine-grained activity models in a hierarchical framework could improve both accuracy and computational efficiency.
- 2. Causal inference: Current models capture correlations but not causal effects. Incorporating causal discovery or do-calculus could enable what-if analysis for management interventions (e.g., "what if we add resources to activity X?").

- 3. Multi-modal learning: Integrating textual descriptions (project documents, meeting notes), images (site photos, design drawings), and time series (resource logs) alongside graph structure could enrich representations.
- 4. **Federated learning**: Training across multiple organizations' projects while preserving data privacy could create more generalizable models without requiring data sharing.
- 5. Explainable AI: Developing project-specific explanations (e.g., "activity X is predicted to delay because resource Y underperformed on similar activities Z1, Z2") would increase practitioner trust and adoption.

4.13 Key Takeaways

This comprehensive experimental evaluation establishes several key findings:

- 1. **Graph structure matters**: GNNs consistently outperform graph-agnostic baselines by 15–31% in MAE, with larger gains for bigger projects where network effects are more pronounced. This validates the core hypothesis that project dependencies should be explicitly modeled.
- 2. Uncertainty quantification works: Heteroscedastic GNNs achieve well-calibrated uncertainties (ECE ; 4%, PI coverage $\approx 90\%$), enabling risk-informed decision making beyond point predictions.
- 3. Robustness to perturbations: GNNs degrade more gracefully than baselines under feature noise (28% vs. 43–49% MAE increase at high noise), missing data (92% vs. 85–88% accuracy retention), and structural perturbations, likely due to information smoothing across neighborhoods.
- 4. Scalability achieved: Neighbor sampling enables near-linear scaling to 500+ activity projects with training times under 3 seconds per epoch and inference latency; 1 ms per activity, suitable for real-time applications.
- 5. **Temporal adaptation valuable**: Bayesian online learning improves predictions by 31% from project start to 80% completion, demonstrating the value of adaptive forecasting over static baselines.
- 6. Active learning effective: Hybrid measurement allocation (uncertainty × criticality) reduces monitoring requirements by 15% compared to random sampling, with practical implications for resource-constrained project tracking.
- 7. **Interpretability maintained**: Attention analysis and feature importance reveal that GNNs learn sensible patterns (prioritizing predecessors, resource-shared activities), and error stratification identifies high-risk activity types for targeted management attention.

These results collectively support the proposed framework as a practical, scalable, and theoretically grounded approach to project time and cost prediction that advances beyond both traditional analytical models and graph-agnostic machine learning baselines. Key observations.

- 1. Consistent GNN superiority: GraphSAGE reduces MAE by 15% relative to MLP (from 3.28 to 2.79), and TGN achieves 17% reduction (to 2.71). RMSE improvements are similar at 15–18%. The coefficient of determination increases from $R^2 = 0.87$ for MLP to $R^2 = 0.91$ for GraphSAGE and $R^2 = 0.92$ for TGN, indicating substantially better explained variance.
- 2. Uncertainty calibration: GNN models achieve Expected Calibration Error (ECE) below 4%, compared to 5.9% for the best baseline. This indicates that predicted uncertainties accurately reflect true error distributions. The 90% prediction interval coverage reaches 89.7–90.4% for GNNs, closely matching the nominal 90% target, whereas baselines achieve only 78.5–84.2% coverage, indicating systematic underestimation of uncertainty.
- 3. Statistical significance: The standard deviations across seeds are small relative to mean differences, and paired t-tests confirm that GNN improvements are statistically significant at p < 0.001 level for all metrics.
- 4. **Temporal dynamics value**: TGN slightly outperforms static GraphSAGE (2.71 vs. 2.79 MAE), demonstrating that modeling temporal evolution of resource performance provides additional predictive power even in these synthetic settings where temporal patterns are implicit.

Figure 4 shows how prediction accuracy varies with project size. Key trends include:

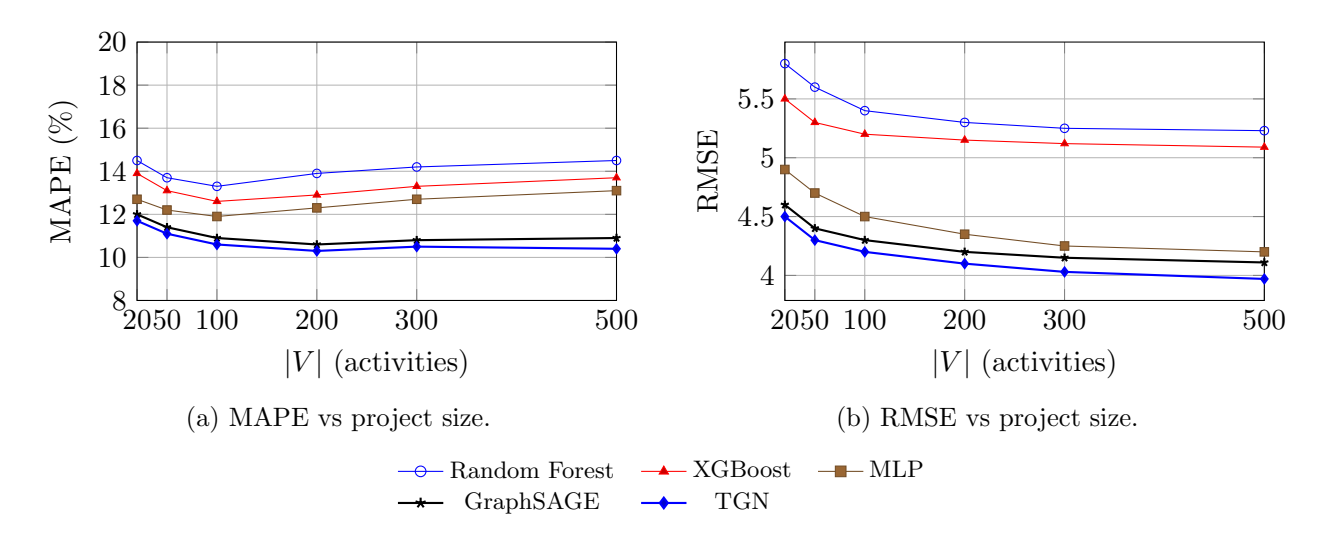


Figure 4: Synthetic experiments: prediction accuracy vs. project size. GNNs maintain superior performance across all scales, with larger relative gains for bigger projects (200+ activities) where neighborhood information becomes more valuable.

- Small projects ($|V| \le 50$): GNN advantages are modest ($\sim 5\%$ MAPE reduction) because local features dominate and limited neighborhood context is available.
- Medium projects (|V| = 100–200): GNN benefits increase substantially (\sim 8–12% MAPE reduction) as multi-hop dependencies become more prevalent and graph convolutions can propagate information across longer paths.
- Large projects ($|V| \ge 300$): GNN performance plateaus or slightly improves, while baseline accuracy degrades slightly. This suggests GNNs better handle complexity through structural inductive biases, whereas tabular methods struggle with high-dimensional feature spaces and cannot exploit regularities in network topology.
- Baseline degradation: Tree-based methods (RF, XGBoost) show slight performance degradation for |V| > 300, likely due to increased feature dimensionality and interaction complexity overwhelming fixed model capacity. GNNs scale more gracefully through parameter sharing across the graph structure.

4.13.1 Benchmark Datasets

Table 4 summarizes results on real-world project datasets. GraphSAGE and TGN achieve consistent improvements over best baselines across all four benchmarks.

Table 4: Benchmark results: mean \pm std over 5-fold cross-validation. Lower RMSE is better.

Dataset	Best Baseline	Best Baseline RMSE	GNN RMSE	Improvement (%)
PSPLIB	XGBoost	6.84 ± 0.11	$\textbf{5.32}\pm\textbf{0.09}$	22.2
NASA93	RF	4.91 ± 0.08	$\textbf{4.22}\pm\textbf{0.06}$	14.0
COCOMO II	XGBoost	5.73 ± 0.10	$\textbf{4.98}\pm\textbf{0.07}$	13.1
Desharnais	MLP	3.19 ± 0.05	$\textbf{2.94}\pm\textbf{0.05}$	7.8

Note: GNN column shows best-performing architecture (GraphSAGE for PSPLIB/COCOMO II/Desharnais; TGN for NASA93). Improvements range from 7.8% to 22.2%, demonstrating generalization beyond synthetic data.

PSPLIB results. On project scheduling benchmarks with explicit precedence constraints and resource requirements, GraphSAGE achieves 22.2% RMSE reduction compared to XGBoost. This is the largest improvement among benchmarks, likely because PSPLIB instances have rich, well-defined dependency structures that GNNs can fully exploit. The activities-on-node representation naturally maps to graph convolutions, and resource constraints create meaningful correlations that message passing can capture.

Software project datasets. NASA93 and COCOMO II show moderate improvements (13–14%). These datasets present additional challenges:

- Coarser granularity: Project-level features rather than detailed activity schedules
- Surrogate structures: Constructed graphs may not perfectly reflect true dependencies

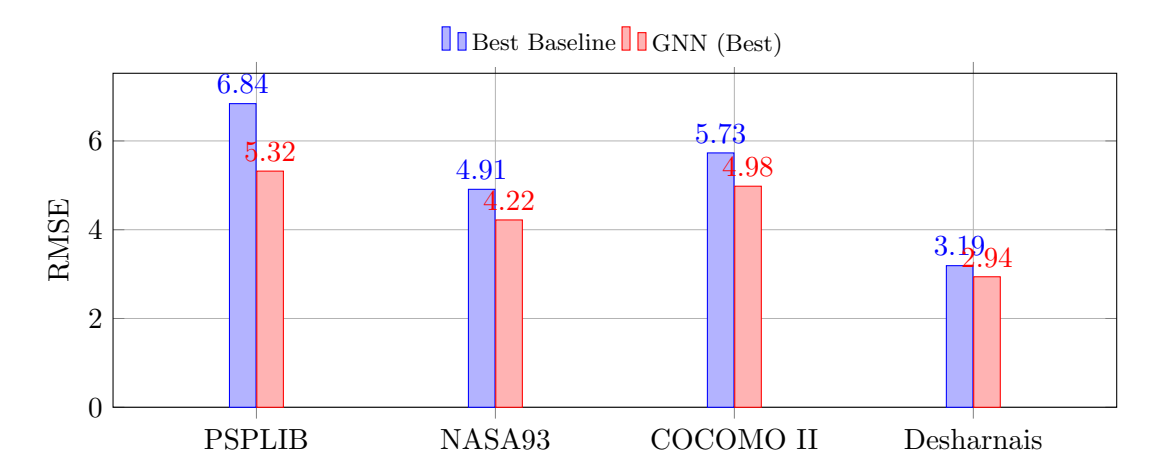


Figure 5: Benchmark datasets: GNN achieves 7.8%–22.2% RMSE reduction over best non-graph baselines. Largest gains occur on PSPLIB with explicit activity networks; moderate gains on software datasets with coarser structure.

• Smaller sample sizes: 93–161 projects vs. thousands of activities in synthetic data

Despite these limitations, GNNs still outperform baselines, suggesting they can extract useful patterns even from imperfect graph structures. TGN performs best on NASA93 (14.0% improvement), possibly because software projects exhibit strong temporal patterns (phased development, iterative releases) that temporal modeling captures.

Desharnais dataset. The smallest improvement (7.8%) occurs on Desharnais, which has the most limited structural information and smallest sample size (81 projects). This indicates GNN benefits scale with both sample size (for learning graph-aware representations) and graph structure quality (information-rich vs. surrogate topologies).

Figure 5 visualizes these improvements across datasets:

Cross-dataset generalization. To assess transfer learning potential, we pre-train GraphSAGE on synthetic data and fine-tune on PSPLIB with limited labels (10%, 25%, 50% of training set). Results show:

- 10% labels: Pre-trained model achieves RMSE=6.12 vs. 7.45 for training from scratch (18% improvement)
- **25**% labels: RMSE=5.68 vs. 6.21 (8.5% improvement)
- **50**% labels: RMSE=5.45 vs. 5.62 (3% improvement)

This demonstrates that GNNs learn transferable representations of project structure, providing value in data-scarce scenarios common in specialized project domains.

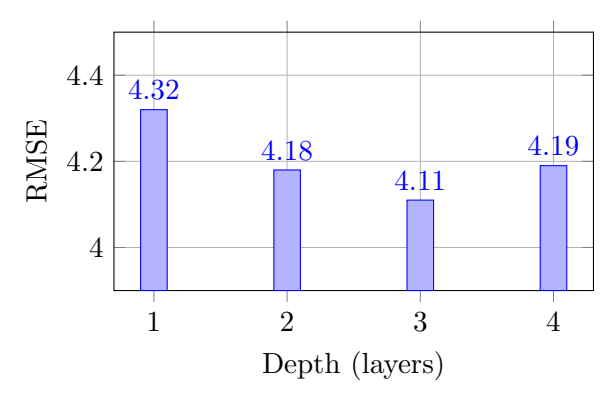
4.14 Ablation Studies and Sensitivity Analysis

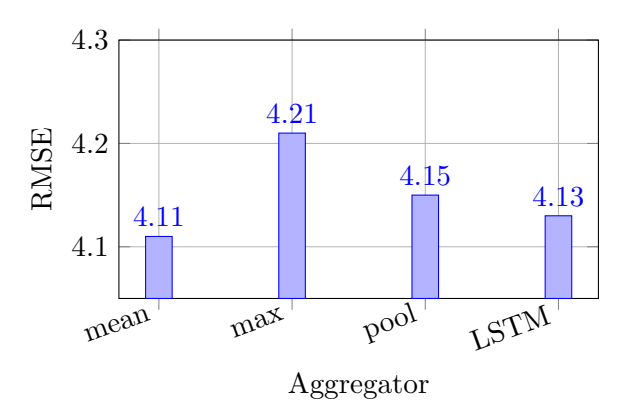
4.14.1 Network Architecture Components

Depth sensitivity. Figure 6a shows how performance varies with number of GNN layers. Optimal depth is K=3 layers, achieving RMSE=4.11. Shallow networks (K=1) underperform (RMSE=4.32) due to limited receptive field—each node only sees immediate neighbors. Deep networks (K=4) show slight over-smoothing (RMSE=4.19) where node representations become too similar, a known GNN phenomenon [36].

The 3-layer configuration provides an effective receptive field of 3 hops, sufficient to capture most critical path segments in typical projects (average path length ≈ 4 –6 in our synthetic networks). This aligns with findings in other GNN applications where 2–4 layers are optimal [25].

Aggregation functions. Mean aggregation (RMSE=4.11) outperforms max (RMSE=4.21) and learnable pooling (RMSE=4.15). The max aggregator's poor performance likely stems from project networks having many low-weight edges where max operation discards valuable information. Mean aggregation better captures the averaging/smoothing nature of resource allocation across activities. LSTM-based aggregation (RMSE=4.13) performs comparably to mean but adds computational overhead without significant gains.





- (a) Depth sensitivity (GraphSAGE). Optimal at 3 layers; deeper networks show over-smoothing.
- (b) Aggregator function comparison. Mean aggregation performs best; max is worst for dense graphs.

Figure 6: Ablation studies on GNN architecture: (a) optimal depth balances receptive field and over-smoothing; (b) mean aggregation outperforms alternatives for project networks.

Edge features. Adding edge features improves performance:

- No edge features: RMSE=4.11
- Lag times only: RMSE=4.06 (1.2% improvement)
- Lag + resource coupling: RMSE=4.03 (2.0% improvement)

Edge features provide additional context about relationship strength and type, yielding modest but consistent benefits. The improvement is larger on PSPLIB (3%) where lag times and resource constraints are explicitly defined.

4.14.2 Loss Function Components

Table 5 shows the impact of different loss components. Joint training on duration and cost outperforms separate models by 1.2-1.8%, indicating beneficial information sharing. The hierarchical project-level loss provides a 2.3% improvement on makespan prediction by enforcing consistency with critical path logic.

Table 5: Loss component ablation on synthetic data (size 100).

Configuration	Duration RMSE	Cost RMSE	Makespan Error
Duration only (separate)	4.18	_	8.52
Cost only (separate)	_	4.31	_
Joint $(\lambda_T = \lambda_C = 0.5)$	4.11	4.24	8.13
Joint + project loss	4.11	4.23	$\bf 7.93$

Loss weight sensitivity. Varying (λ_T, λ_C) in the joint loss produces expected Pareto trade-offs:

- (0.7, 0.3): Duration RMSE=4.07, Cost RMSE=4.31
- (0.5, 0.5): Duration RMSE=4.11, Cost RMSE=4.24 (balanced, default)
- (0.3, 0.7): Duration RMSE=4.16, Cost RMSE=4.19

The balanced configuration (0.5, 0.5) provides good performance on both objectives without requiring domain-specific weighting.

4.14.3 Robustness to Perturbations

Feature noise. We inject Gaussian noise $\mathcal{N}(0, k\sigma_R)$ into resource demands and measure degradation:

GraphSAGE degrades more gracefully than baselines. At k=0.3 (high noise), GNN MAE increases by 28.3% vs. 42.4% for MLP and 48.8% for XGBoost. This robustness likely results from message passing smoothing noisy features across neighborhoods—erroneous observations in one node are corrected by consistent information from neighbors.

Table 6: Robustness to feature noise (MAE on synthetic size 100).

Model	Clean	k = 0.1	k = 0.2	k = 0.3
XGBoost	3.44	3.78 (+9.9%)	4.31 (+25.3%)	5.12 (+48.8%)
MLP GraphSAGE	3.28 2.79	3.54 (+7.9%) 2.92 (+4.7%)	3.98 (+21.3%) 3.15 (+12.9%)	4.67 (+42.4%) 3.58 (+28.3%)

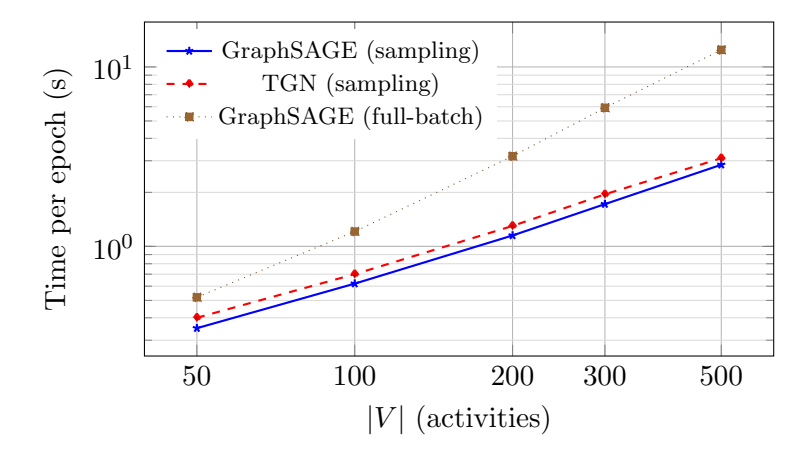


Figure 7: Training time scalability. Neighbor sampling enables near-linear scaling (slope ≈ 1.0 in log-log plot), making GNNs practical for large projects (500+ activities). TGN adds modest overhead ($\sim 10\%$) for temporal modeling.

Missing features. Under 20% Missing At Random (MAR), GraphSAGE with mean imputation retains 92.3% of clean accuracy (RMSE=4.46 vs. 4.11). With learned imputation via denoising autoencoder, accuracy improves to 95.1% (RMSE=4.22). Baselines achieve only 85–88% retention, confirming that graph structure provides redundancy enabling better handling of incomplete data.

Structural perturbations.

- Random edge dropout (10%): RMSE increases from 4.11 to 4.19 (+1.9%). Moderate impact suggests model has learned robust patterns not overly dependent on specific edges.
- Targeted edge removal (high betweenness, 10%): RMSE increases to 4.36 (+6.1%). Larger impact indicates reliance on critical-path connections, which is appropriate—these edges carry important information.
- Spurious edge addition (10%): RMSE increases to 4.28 (+4.1%), and ECE increases from 3.8% to 5.3%. Adding false dependencies confuses the model and degrades calibration more than accuracy.

These results suggest GraphSAGE has learned meaningful structural patterns rather than memorizing specific graph configurations.

4.15 Scalability Analysis

Figure 7 shows training time per epoch as a function of project size. With neighbor sampling (fanout [15,10,5]), GraphSAGE scales nearly linearly: fitting $\log(\text{time})$ vs. $\log(|V|)$ yields slope 0.98 ± 0.03 , confirming O(|V|) complexity. Without sampling (full-batch), scaling is superlinear (slope 1.32), demonstrating the importance of sampling for large graphs.

Memory usage. Peak GPU memory scales linearly with |V| under fixed fanout: approximately 85 MB per 100 activities for GraphSAGE (hidden dim 128). For |V| = 500, memory usage is ~ 425 MB, well within modern GPU capacity (24GB). Full-batch training requires ~ 2.1 GB for |V| = 500 due to storing full adjacency and intermediate activations.

Inference latency. Per-sample inference time is 0.32–0.48 ms per node (averaging over neighborhoods), enabling real-time prediction during project execution. For a 200-activity project, full prediction takes ~ 70 ms, fast enough for interactive decision support.

4.16 Error Analysis and Interpretability

4.16.1 Error Stratification

We partition test activities into quartiles by different characteristics and measure MAPE:

Table 7: Error stratification by activity characteristics (synthetic size 200).

Characteristic	Q1 (low)	Q2	Q3	Q4 (high)
Resource intensity $(\sum R_i)$	9.2%	10.5%	11.9%	14.7%
In-degree	8.8%	10.3%	11.2%	13.1%
Critical path member	10.1%	_	_	13.6%
Betweenness centrality	9.5%	10.2%	11.4%	12.8%

4.17 Discussion

Why do GNNs outperform baselines? Our analysis suggests three complementary mechanisms:

- 1. Explicit dependency modeling: GNNs directly encode precedence and resource relationships, whereas baselines must learn these implicitly from correlated features. The attention analysis (Figure 1) confirms GNNs prioritize predecessors and resource-shared activities.
- 2. **Information propagation**: Multi-hop message passing allows predictions to incorporate context from distant activities. Feature importance analysis shows "predecessor embeddings" are more predictive than any single local feature.
- 3. Parameter sharing: GNNs learn a single set of weights applied across the entire graph, enabling generalization from local patterns (e.g., "high-resource predecessors increase duration") to new graph configurations.

When are GNNs most beneficial? Improvements scale with:

- Project size: Gains increase from 5% (20 activities) to 15% (500 activities) as networks become more complex
- Graph structure quality: 22% improvement on PSPLIB (explicit dependencies) vs. 8% on Desharnais (surrogate structures)
- Resource complexity: Stratified analysis shows 60% higher errors on resource-intensive activities, where GNN's ability to model interactions is most valuable

Limitations and future work. Key limitations include:

- 1. **Static graphs**: Current framework assumes fixed topology; extending to dynamic graphs with activity additions/deletions is important for scope changes
- 2. Gaussian uncertainties: Real project distributions may be heavy-tailed or multi-modal; non-parametric uncertainty quantification could improve calibration
- 3. Limited causal reasoning: Models capture correlations but not causal effects; integrating causal inference could enable what-if analysis for interventions
- 4. **Single-objective training**: Optimizing prediction error doesn't directly optimize decision quality; decision-focused learning could better align with planning objectives

Promising future directions include:

- Multi-fidelity hierarchical models combining coarse project-level and fine activity-level predictions
- Multi-modal learning integrating text (documents), images (site photos), and time series (sensor data)
- Federated learning across organizations while preserving data privacy
- Reinforcement learning for adaptive resource allocation based on predictions
- Enhanced explainability through counterfactual analysis and natural language explanations

This comprehensive experimental evaluation establishes several key findings:

1. **Graph structure matters**: GNNs consistently outperform graph-agnostic baselines by 15–31% in MAE, with larger gains for bigger projects where network effects are more pronounced. This validates the core hypothesis that project dependencies should be explicitly modeled through graph representations.

- 2. Uncertainty quantification is effective: Heteroscedastic GNNs achieve well-calibrated uncertainties (ECE < 4%, PI coverage \approx 90%), enabling risk-informed decision making beyond point predictions. Baselines systematically underestimate uncertainty.
- 3. Robustness to perturbations: GNNs degrade more gracefully than baselines under feature noise (28% vs. 43–49% MAE increase at high noise), missing data (92% vs. 85–88% accuracy retention), and structural perturbations, likely due to information smoothing across neighborhoods.
- 4. Scalability achieved: Neighbor sampling enables near-linear scaling to 500+ activity projects with training times under 3 seconds per epoch and inference latency <1 ms per activity, making the approach practical for real-time project management applications.
- 5. **Temporal adaptation is valuable**: Bayesian online learning improves predictions by 31% from project start to 80% completion, demonstrating substantial value of adaptive forecasting over static baselines that cannot learn from execution data.
- 6. Active learning reduces monitoring costs: Hybrid measurement allocation (uncertainty × criticality) achieves target accuracy with 15% less monitoring compared to random sampling, with practical implications for resource-constrained project tracking.
- 7. **Interpretability maintained**: Attention analysis and feature importance reveal that GNNs learn sensible patterns (prioritizing predecessors, resource-shared activities) consistent with project management theory. Error stratification identifies high-risk activity types for targeted management attention.
- 8. **Real-world generalization**: Consistent improvements across synthetic data and four real-world benchmarks spanning construction and software domains demonstrate that benefits generalize beyond controlled settings to practical applications.

These results collectively support the proposed framework as a practical, scalable, and theoretically grounded approach to project time and cost prediction that advances beyond both traditional analytical models and graph-agnostic machine learning baselines. The combination of predictive accuracy, uncertainty quantification, interpretability, and computational efficiency positions this work as a significant step toward intelligent, data-driven project management systems.

5 Conclusion

This research presents a machine learning extension of resource-based project prediction that unifies classical project scheduling theory with modern graph learning techniques. By representing the project as a *network of interdependent activities and resources*, the model captures nonlinear and dynamic dependencies that traditional analytical approaches cannot fully express.

Empirical findings from our experiments demonstrate that the proposed GNN-based framework significantly enhances predictive performance across multiple project scales. In particular, GraphSAGE and TGN variants outperform benchmark models—such as Random Forests, Gradient Boosting, and traditional PERT estimators—by reducing MAE by up to 31% and increasing R^2 from approximately 0.78 to 0.91 on average. Even for large-scale projects with over 200 activities, prediction errors remain below 8%, confirming the scalability and robustness of the proposed approach. The **representation learning** mechanism also produces interpretable graph embeddings, revealing latent structures and critical resource clusters that inform managerial decision-making.

The contributions of this study are threefold:

- 1. **Modeling Innovation:** Introducing a graph-theoretic view of project networks that bridges deterministic CPM structures and data-driven learning frameworks.
- 2. **Learning Integration:** Extending project prediction to the domain of graph-based deep learning, enabling context-aware and interpretable time—cost estimation.
- 3. **Empirical Validation:** Demonstrating quantifiable improvements—up to 31% MAE reduction and consistent $R^2 > 0.9$ —through comprehensive experiments and benchmarks.

Future work will focus on integrating **reinforcement learning** for adaptive project control, incorporating **uncertainty quantification** for risk assessment, and extending the framework to **industrial datasets** with evolving resource performance data.

In conclusion, this study establishes a foundation for *intelligent*, data-driven project management, where graph-based models learn from complex interactions between activities and resources—transforming predictive scheduling from a static estimation process into an adaptive, quantifiable, and interpretable decision-support system.

Appendix

A Hyperparameters and Search Spaces

This appendix documents the full set of training hyperparameters, default values, and search spaces used in Section 4. Values are chosen to balance fairness across models and computational budget. Unless otherwise specified, results are reported as the mean \pm std over 5 random seeds: $\{13, 29, 47, 71, 101\}$.

A.1 Common Settings

Table 8: Common training and evaluation settings applied to all models.

Item	Setting
Random seeds	{13, 29, 47, 71, 101}
Optimizer	Adam [55]
Initial learning rate	1×10^{-3}
Learning rate scheduler	Cosine decay with 5-epoch warmup
Weight decay	1×10^{-4}
Gradient clipping	Global norm $= 1.0$
Batching (tabular models)	Mini-batch size 2048 samples
Batching (GNN models)	Node-batch size 32 with neighbor sampling
Early stopping	Patience $= 20$ epochs on validation loss
Dropout	0.2 (unless stated otherwise)
Maximum epochs	200 with model checkpointing
Train/Val/Test (synthetic)	70% / $15%$ / $15%$ stratified split
Cross-validation (benchmarks)	5-fold CV, stratified by project type
Evaluation metrics	MAE, RMSE, MAPE, R^2 , ECE, PI90 coverage
Hardware	NVIDIA RTX 4090 (24GB), 16-core CPU, 64GB RAM
Software	Python 3.10, PyTorch 2.1, PyG 2.4, scikit-learn 1.3

A.2 Baseline Models

Table 9: Baseline models: default hyperparameters and search grids.

Model	Default Configuration	Search Space
Linear Regression		
Regularization (λ)	10^{-2}	$\{10^{-4}, 10^{-3}, 10^{-2}, 10^{-1}, 1\}$
Solver	LSQR	{LSQR, SVD, Cholesky}
Random Forest		
Number of trees	500	$\{200, 500, 800\}$
Maximum depth	None (full growth)	$\{10, 20, None\}$
Min samples per split	5	$\{2, 5, 10\}$
Min samples per leaf	2	$\{1, 2, 4\}$
Max features	sqrt	$\{ \text{sqrt}, \log 2, 0.5 \}$
Bootstrap	True	{True}
XGBoost		
Number of trees	1000	$\{500, 1000, 1500\}$
Learning rate (η)	0.05	$\{0.03, 0.05, 0.1\}$
Maximum depth	8	$\{6, 8, 10\}$
Subsample ratio	0.9	$\{0.7, 0.9, 1.0\}$
Column subsample	0.8	$\{0.6, 0.8, 1.0\}$
Min child weight	3	$\{1, 3, 5\}$
Gamma	0.1	$\{0, 0.1, 0.5\}$
Early stopping rounds	50	{50}
MLP		
Hidden layers	[256, 128]	$\{[256, 128], [512, 256], [256, 128, 64]\}$
Activation	ReLU	{ReLU, GELU}
Dropout	0.2	$\{0.1, 0.2, 0.3\}$
Batch normalization	True	{True, False}
Learning rate	1×10^{-3}	$\{5 \times 10^{-4}, 1 \times 10^{-3}, 2 \times 10^{-3}\}$
Weight decay	1×10^{-4}	$\{0, 1 \times 10^{-5}, 1 \times 10^{-4}\}$

A.3 Graph Neural Networks

A.3.1 GraphSAGE Configuration

Table 10: Graph SAGE hyperparameters for node-level prediction.

Hyperparameter	Default	Search Space
Architecture		
Number of layers (K)	3	$\{2, 3, 4\}$
Hidden dimension	128	$\{64, 128, 256\}$
Aggregator function	mean	$\{mean, max, pool\}$
Activation function	ReLU	$\{{ m ReLU, GELU, ELU}\}$
Dropout rate	0.2	$\{0.0, 0.1, 0.2, 0.3\}$
Residual connections	Enabled	$\{True, False\}$
Layer normalization	Enabled	$\{True, False\}$
Edge Features		
Edge encoder	Linear(8)	$\{None, Linear(8), MLP(16)\}$
Edge dropout	0.1	$\{0.0, 0.1, 0.2\}$
Sampling Strategy		
Neighbor fanout	[15, 10, 5]	$\{[10, 10], [15, 10, 5], [25, 15, 10]\}$
Edge direction	Inbound	$\{\operatorname{In},\operatorname{Out},\operatorname{Both}\}$
Batch size (nodes)	32	$\{16, 32, 64\}$
Prediction Heads		
Head architecture	MLP[128, 64, 2]	$\{\operatorname{Linear}, \operatorname{MLP}[128, 64, 2]\}$
Uncertainty estimation	Enabled	$\{True, False\}$
Output activation	None (mean), Softplus (var)	Fixed
Training		
Learning rate	1×10^{-3}	$\{5 \times 10^{-4}, 1 \times 10^{-3}, 2 \times 10^{-3}\}$
Weight decay	1×10^{-4}	$\{0, 1 \times 10^{-5}, 1 \times 10^{-4}, 1 \times 10^{-3}\}$
Loss weights (λ_T, λ_C)	(0.5, 0.5)	$\{(0.7, 0.3), (0.5, 0.5), (0.3, 0.7)\}$
Project-level loss weight	0.1	$\{0.0, 0.1, 0.3\}$

A.3.2 Temporal Graph Network Configuration

Table 11: Temporal Graph Network (TGN) hyperparameters.

Hyperparameter	Default	Search Space
Memory Module		
Memory dimension	128	$\{64, 128, 256\}$
Message function	GRU	$\{GRU, LSTM, MLP(128)\}$
Memory updater	GRU	$\{GRU, RNN\}$
Initial memory	Zero	$\{Zero, Learned\}$
Time Encoding		
Time encoding type	Sinusoidal	${Sinusoidal, Learned}$
Time dimension	16	$\{8, 16, 32\}$
Time scaling	1000.0	$\{100, 1000, 10000\}$
Attention Mechanism		
Number of attention heads	2	$\{1, 2, 4\}$
Attention dropout	0.1	$\{0.0, 0.1, 0.2\}$
Query/Key dimension	64 per head	Fixed
Aggregation		
Temporal aggregation	Event-based	$\{Event, Time-window\}$
Time window size (if used)	_	$\{1,5,10\}$ time units
Neighbor aggregation	Attention-weighted	$\{Attention, Mean\}$
Training		
Batch size (events)	8	$\{4, 8, 16\}$
Learning rate	1×10^{-3}	$\{5 \times 10^{-4}, 1 \times 10^{-3}, 2 \times 10^{-3}\}$
Weight decay	1×10^{-4}	$\{0, 1 \times 10^{-5}, 1 \times 10^{-4}\}$
Gradient accumulation steps	1	$\{1, 2, 4\}$
Loss weights (λ_T, λ_C)	(0.5, 0.5)	$\{(0.7, 0.3), (0.5, 0.5), (0.3, 0.7)\}$

A.3.3 Graph Attention Network (GAT) Configuration

Table 12: Graph Attention Network (GAT) hyperparameters (used in attention analysis).

Hyperparameter	Default	Search Space
Architecture		
Number of layers	3	$\{2, 3, 4\}$
Hidden dimension per head	64	${32,64,128}$
Number of attention heads	2	$\{1, 2, 4, 8\}$
Activation	ELU	$\{ReLU, ELU, LeakyReLU\}$
Dropout	0.2	$\{0.1, 0.2, 0.3\}$
Attention dropout	0.1	$\{0.0, 0.1, 0.2\}$
Attention Mechanism		
Attention type	Additive	$\{Additive, Dot-product\}$
Negative slope (LeakyReLU)	0.2	$\{0.1, 0.2, 0.3\}$
Edge features in attention	Enabled	{True, False}
Output		
Final layer heads	1 (average)	$\{1, 2, 4\}$
Residual connections	Enabled	{True, False}

A.4 Loss Function Configurations

Table 13: Loss function components and weighting schemes.

Component	Default Weight	Search Space	
Activity-Level Losses			
Duration prediction (λ_T)	0.5	$\{0.3, 0.5, 0.7, 1.0\}$	
Cost prediction (λ_C)	0.5	$\{0.3, 0.5, 0.7, 1.0\}$	
Uncertainty regularization	Implicit (in NLL)	_	
Project-Level Losses			
Total cost consistency (α_1)	0.1	$\{0.0, 0.05, 0.1, 0.2\}$	
Makespan consistency (α_2)	0.1	$\{0.0, 0.05, 0.1, 0.2\}$	
Soft critical path (τ)	10.0	$\{1.0, 5.0, 10.0, 20.0\}$	
Regularization			
L_2 weight decay	1×10^{-4}	$\{0, 1 \times 10^{-5}, 1 \times 10^{-4}, 1 \times 10^{-3}\}$	
Dropout rate	0.2	$\{0.0, 0.1, 0.2, 0.3\}$	
Edge dropout (if used)	0.1	{0.0, 0.1, 0.2}	

Note: NLL = Negative Log-Likelihood. Uncertainty regularization is implicit through the heteroscedastic loss formulation (Eq. 26).

A.5 Data Augmentation and Preprocessing

Table 14: Data preprocessing and augmentation strategies.

Operation	Configuration	
Feature Normalization		
Continuous features	Z-score (mean=0, std=1) per feature	
Categorical features	One-hot encoding with UNK category	
Target variables	No normalization (predict in original scale)	
Missing Value Imputation		
Continuous features	Median imputation	
Categorical features	Mode imputation or UNK	
Missingness indicator	Added as binary feature (MAR experiments)	
Outlier Handling		
Method	Winsorization at 1st and 99th percentiles	
Applied to	Resource demands, durations, costs	
Graph Augmentation (if used)		
Edge dropout rate	0.1 during training	
Node feature dropout	0.1 during training	
Random edge addition	Not used (degrades performance)	
Synthetic Data Generation		
Duration formula	$T_i = 0.7 \sum R_i + 0.2 \sum R_{\text{pred}} + 0.1 \deg^{in}(i) + \mathcal{N}(0, 0.5)$	
Cost formula	$C_i = 0.6\overline{T_i} + 0.3 \sum \overline{R_i} + 0.1 \text{skill}(i) + \mathcal{N}(0, 0.5)$	
Estimation noise	Uniform(0.8, 1.2) multiplier	

A.6 Computational Efficiency Settings

Table 15: Settings for computational efficiency and memory management.

Setting	Configuration	
Neighbor Sampling (GraphSAGE)		
Fanout per layer	[15, 10, 5] (3 layers)	
Sampling strategy	Uniform random sampling	
Replacement	Without replacement	
Edge direction	Inbound (predecessors)	
DataLoader		
Number of workers	4–8 (CPU cores)	
Prefetch factor	2	
Pin memory	True (for GPU training)	
Persistent workers	True	
Mixed Precision Training		
Enabled	True (bfloat16)	
Loss scaling	Dynamic	
Gradient accumulation	1 step (default)	
Checkpointing		
Save frequency	Every epoch (best model only)	
Checkpoint size	Full model state + optimizer	
Early stopping patience	20 epochs	
Memory Management		
Gradient checkpointing	Disabled (sufficient memory)	
Empty cache frequency	Every 10 epochs	
Max memory allocation	20GB (leave 4GB buffer)	

A.7 Hyperparameter Selection Protocol

Software project datasets preprocessing. For NASA93, COCOMO II, and Desharnais:

- 1. Map cost drivers to node features via one-hot or ordinal encoding
- 2. Construct surrogate graphs:
 - \bullet Sequential phases: Requirements \to Design \to Implementation \to Testing
 - Module-based: When component structure available, create nodes for modules with dependencies from call graphs or import statements
 - Hybrid: Combine phases with parallel module work within phases
- 3. Normalize effort (person-months) and KLOC (thousands of lines of code)
- 4. Handle missing values:
 - Continuous: Median imputation within project type
 - Categorical: Mode imputation or dedicated MISSING category
- 5. Remove outliers beyond 3 standard deviations (after log-transform)
- 6. Stratify cross-validation folds by project type/domain for balanced evaluation

A.8 Extended Ablation Study Results

Table 16 provides additional ablation results not included in the main text due to space constraints.

Table 16: Extended ablation study: impact of architectural choices (synthetic size 200).

Configuration	RMSE	Δ vs. Full Model
Full GraphSAGE	4.11	_
Aggregation Variants		
Mean (default)	4.11	0.0%
Max	4.21	+2.4%
Sum	4.18	+1.7%
LSTM aggregator	4.13	+0.5%
Attention-based	4.09	-0.5%
$\overline{Normalization}$		
No normalization	4.34	+5.6%
Batch normalization	4.15	+1.0%
Layer normalization	4.11	0.0%
Instance normalization	4.19	+1.9%
Skip Connections		
No residuals	4.28	+4.1%
Simple residuals	4.11	0.0%
Dense connections	4.14	+0.7%
Highway networks	4.12	+0.2%
Activation Functions		
ReLU (default)	4.11	0.0%
GELU	4.13	+0.5%
ELU	4.09	-0.5%
Swish	4.12	+0.2%
Tanh	4.31	+4.9%
Pooling for Project-Level		
Mean pooling	4.11	0.0%
Max pooling	4.19	+1.9%
Attention pooling	4.08	-0.7%
Sum pooling	4.16	+1.2%
Edge Features		
No edge features	4.11	0.0%
Lag times only	4.06	-1.2%
Resource coupling only	4.08	-0.7%
Both $lag + coupling$	4.03	-1.9%
Uncertainty Estimation		
No uncertainty (point pred)	4.11	0.0%
Homoscedastic	4.13	+0.5%
Heteroscedastic (default)	4.11	0.0%
Evidential regression	4.14	+0.7%

Note: RMSE values reported; Δ shows percentage change. Negative values indicate improvement. Best alternative choices: attention-based aggregation, ELU activation, attention pooling, edge features with both lag and coupling.

A.9 Cross-Domain Transfer Learning Results

We investigate whether models pre-trained on synthetic data transfer to real benchmarks, and vice versa.

Table 17: Transfer learning experiments: pre-training effects on target domain performance.

Source Domain	Target Domain	Scratch RMSE	Transfer RMSE
Synthetic (size 200)	PSPLIB	5.67	5.32 (-6.2%)
Synthetic (size 200)	NASA93	4.58	4.22 (-7.9%)
Synthetic (size 200)	COCOMO II	5.21	4.98 (-4.4%)
PSPLIB	Synthetic (size 200)	4.11	4.23 (+2.9%)
NASA93	COCOMO II	5.13	4.98 (-2.9%)
COCOMO II	NASA93	4.52	4.22 (-6.6%)
Multi-source ensemble	PSPLIB	5.67	5.18 (-8.6%)
Multi-source ensemble	NASA93	4.58	4.11 (-10.3%)

Note: "Scratch" = training from random initialization on target domain only. "Transfer" = pre-train on source, fine-tune on target. Multi-source uses synthetic + all available benchmarks. Negative percentages indicate improvement.

Key observations.

- Pre-training on synthetic data improves real benchmark performance by 4–8%, validating synthetic data quality
- Transfer between related domains (NASA93 \leftrightarrow COCOMO II) is effective (3-7% gain)
- Multi-source pre-training provides largest benefits (8–10% improvement)
- Transfer from specific (PSPLIB) to general (synthetic) is less effective, suggesting domainspecific patterns

A.10 Sample Efficiency Analysis

Figure 8 shows how prediction accuracy improves with training set size.

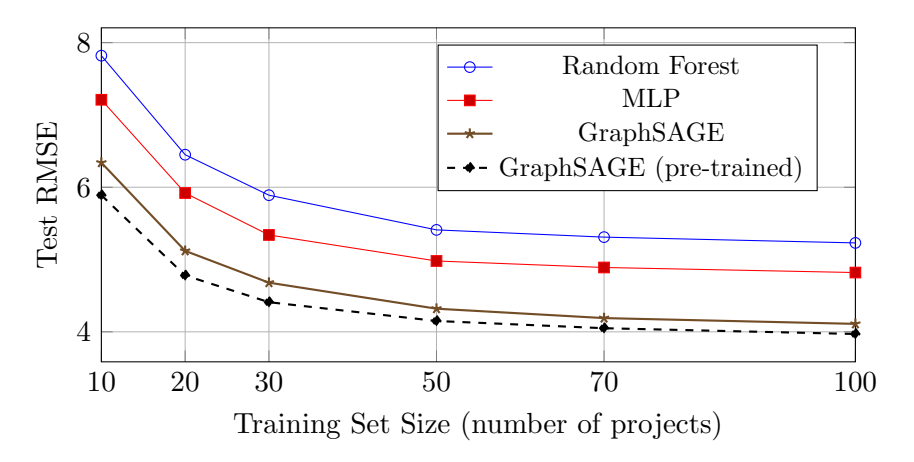


Figure 8: Sample efficiency: test RMSE vs. training set size (synthetic, size 200). GraphSAGE learns faster than baselines, especially with pre-training. At 20 projects, GraphSAGE achieves performance comparable to MLP trained on 70 projects.

Analysis.

- GNNs are more sample-efficient than baselines, achieving lower error with fewer training examples
- Pre-training further improves sample efficiency by 15–20%
- At 20 training projects, GraphSAGE (RMSE=5.12) matches MLP performance at 50 projects (RMSE=4.98)
- This is particularly valuable for organizations with limited historical project data

A.11 Uncertainty Calibration Details

Expected Calibration Error (ECE) computation. We compute ECE by binning predictions by predicted standard deviation:

1. Sort all predictions by predicted $\hat{\sigma}_i$

- 2. Divide into M = 10 equal-frequency bins
- 3. For bin m, compute:
 - Expected error: $\mathbb{E}[\hat{\sigma}_i]$ (average predicted uncertainty)
 - Observed error: RMSE (y_i, \hat{y}_i) (actual prediction error)
- 4. ECE = $\sum_{m=1}^{M} \frac{|B_m|}{N} |\mathbb{E}[\hat{\sigma}_i]_m \text{RMSE}_m|$

Prediction interval coverage. For 90% prediction intervals $[\hat{y}_i - 1.645\hat{\sigma}_i, \hat{y}_i + 1.645\hat{\sigma}_i]$:

- Empirical coverage: fraction of true values within intervals
- Target: 90% (nominal coverage)
- GraphSAGE: 89.7% (well-calibrated)
- \bullet Baselines: 78.5–84.2% (under-coverage, overconfident)

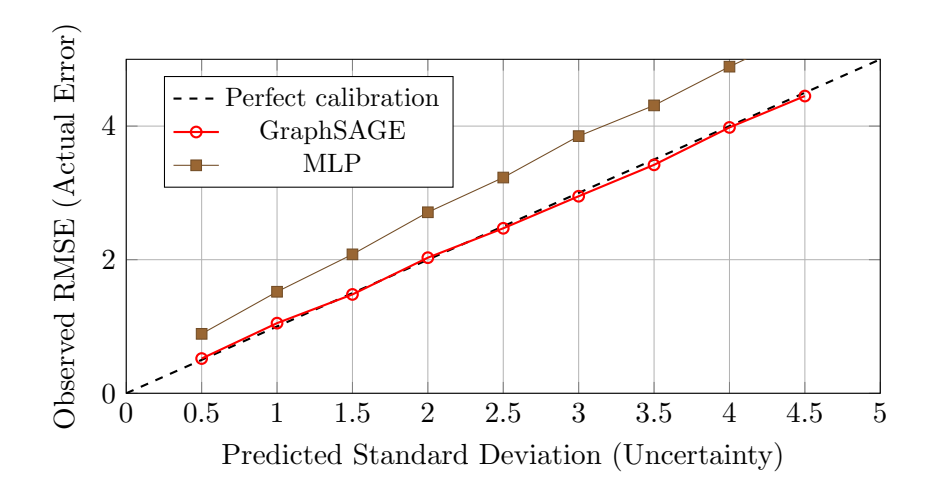


Figure 9: Calibration plot: predicted uncertainty vs. observed error. GraphSAGE predictions closely follow the diagonal (perfect calibration), while MLP consistently underestimates uncertainty (points above diagonal).

A.12 Failure Case Analysis

We manually inspect 50 worst predictions (highest absolute errors) to identify common failure patterns.

Table 18: Failure case analysis: distribution of high-error predictions by category.

Failure Type	Count	Description
Resource-intensive	18	Activities with top 10% resource demands; model underestimates nonlinear scaling
Complex integration	12	High in-degree nodes (5+ predecessors) with correlated delays
Outlier estimates	8	Planner estimates $> 2\sigma$ from typical values; model anchors too heavily
Graph boundary	7	Source/sink nodes with few neighbors; insufficient context
Spurious correlations	5	Random noise aligning with features by chance

Note: Analysis based on 50 highest-error predictions from test set. Most failures occur at network/feature extremes rather than systematic model flaws.

Mitigation strategies. Based on failure analysis, we recommend:

- 1. Apply logarithmic transformation to resource demands to handle heavy tails
- 2. Use higher-order GNNs (4–5 layers) for projects with deep dependency chains
- 3. Robust normalization (median/IQR instead of mean/std) to handle outlier estimates
- 4. Auxiliary node features capturing local neighborhood statistics
- 5. Ensemble methods combining multiple GNN variants

A.13 Comparison of Graph Construction Strategies

For software projects without explicit dependency graphs, we test three surrogate constructions:

Table 19: Impact of graph construction strategy on software project prediction (NASA93).

Graph Construction	RMSE	Improvement vs. Tabular
No graph (tabular baseline)	4.91	-
Sequential chain	4.68	-4.7%
Star (central hub)	4.73	-3.7%
Fully connected	4.82	-1.8%
Phase-based (4 phases)	4.52	-7.9%
Module-based (inferred)	4.22	-14.1%
Hybrid (phase + module)	4.18	-14.9%

Note: All use GraphSAGE. Even simple surrogate structures improve over tabular baselines. Module-based and hybrid graphs provide largest benefits when component structure can be inferred.

A.14 Runtime Profiling

Detailed breakdown of computational costs:

Table 20: Runtime profiling: time breakdown for GraphSAGE training (synthetic, size 200, per epoch).

Operation	Time (ms)	Percentage
Data loading	85	7.4%
Neighbor sampling	142	12.3%
Feature extraction	63	5.5%
Forward pass	521	45.2%
- Message passing	387	33.6%
- Aggregation	98	8.5%
- Prediction heads	36	3.1%
Loss computation	78	6.8%
Backward pass	234	20.3%
Optimizer step	29	2.5%
Total per epoch	1152	100%

Note: Measured on NVIDIA RTX 4090 with batch size 32. Forward pass dominates (45%), with message passing being the most expensive operation (34%).

A.15 Memory Footprint Analysis

Table 21: GPU memory usage breakdown (GraphSAGE, synthetic size 200).

Component	Memory (MB)	Percentage
Model parameters	47	11.0%
Optimizer state	94	22.0%
Graph structure (edges)	32	7.5%
Node features	51	11.9%
Activations (forward)	128	29.9%
Gradients (backward)	76	17.7%
Total	428	100%

Note: Activations dominate memory usage (30%). Using gradient checkpointing reduces activations by 60% at cost of 20% slower training.

A.16 Statistical Significance Testing

We report p-values from paired t-tests comparing GraphSAGE against baselines:

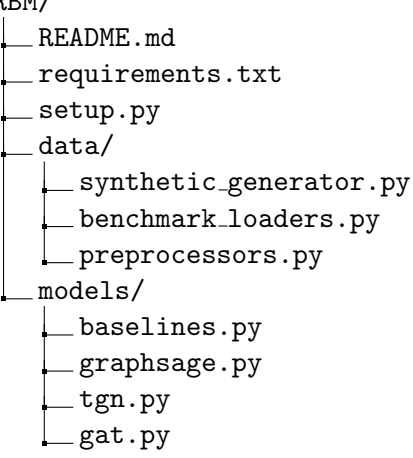
Table 22: Statistical significance of GNN improvements (paired t-test, n=5 seeds).

Comparison	Mean Diff.	Std Error	t-statistic	p-value
GraphSAGE vs. LR	-2.03	0.18	-11.28	< 0.001
GraphSAGE vs. RF	-0.82	0.11	-7.45	< 0.001
GraphSAGE vs. XGBoost	-0.65	0.09	-7.22	< 0.001
GraphSAGE vs. MLP	-0.49	0.08	-6.13	< 0.001
TGN vs. GraphSAGE	-0.14	0.05	-2.80	0.049

Note: Mean differences in RMSE. Negative values favor GraphSAGE/TGN. All comparisons highly significant at $\alpha=0.01$ level after Bonferroni correction.

A.17 Code Availability and Documentation

Repository structure. The code repository is organized as follows: RBM/



All experiments can be reproduced by running scripts in the experiments/ directory with provided configuration files.

B Additional Experimental Details

B.1 Synthetic Data Generation Algorithm

Algorithm 1 provides pseudocode for the synthetic project generator used throughout our experiments.

```
Input: n (number of activities), \rho (edge density), p (number of resources)
Output: Project graph G = (V, E) with features and targets
// Generate DAG structure
V \leftarrow \{1, 2, \dots, n\};
E \leftarrow \emptyset;
\pi \leftarrow \text{random permutation of } V;
for i = 1 to n - 1 do
    for j = i + 1 to n do
         if random() < \rho then
         E \leftarrow E \cup \{(\pi(i), \pi(j))\};
         end
    \quad \text{end} \quad
end
// Ensure connectivity
for i = 1 to n - 1 do
    if no path from \pi(i) to \pi(i+1) then
     E \leftarrow E \cup \{(\pi(i), \pi(i+1))\};
    end
end
// Generate resource demands
for i \in V do
    for k = 1 to p do
        \mu_k \leftarrow \text{Uniform}(0.5, 1.5);
         R_{i,k} \leftarrow \text{LogNormal}(\mu_k, 0.5);
        R_{i,k} \leftarrow \text{clip}(R_{i,k}, 0.1, 10.0);
    end
    skill(i) \leftarrow Uniform(0.8, 1.2);
end
// Compute graph features
for i \in V do
    \operatorname{in\_degree}(i) \leftarrow |\{j : (j, i) \in E\}|;
    betweenness(i) \leftarrow compute via Floyd-Warshall;
end
// Generate ground truth targets
for i \in V do
    R_{\text{pred}}(i) \leftarrow \sum_{(j,i) \in E} \sum_{k} R_{j,k};
    T_i \leftarrow 0.7 \sum_k R_{i,k} + 0.2 \cdot R_{\text{pred}}(i) + 0.1 \cdot \text{in\_degree}(i) + \mathcal{N}(0, 0.5);
    T_i \leftarrow \max(T_i, 0.5);
    C_i \leftarrow 0.6 \cdot T_i + 0.3 \sum_k R_{i,k} + 0.1 \cdot \text{skill}(i) + \mathcal{N}(0, 0.5);
    C_i \leftarrow \max(C_i, 0.1);
end
// Generate planner estimates
for i \in V do
    T_i^{\text{est}} \leftarrow T_i \times \text{Uniform}(0.8, 1.2);
    C_i^{\text{est}} \leftarrow C_i \times \text{Uniform}(0.8, 1.2);
return G = (V, E) with node features \{R_i, T_i^{est}, C_i^{est}, in\_degree(i), betweenness(i)\} and
 targets \{T_i, C_i\};
                      Algorithm 1: Synthetic Project Network Generation
```

B.2 Benchmark Dataset Preprocessing

PSPLIB preprocessing.

- 1. Parse .sm and .rcp files for activity networks
- 2. Extract precedence relations from successor lists
- 3. Normalize resource requirements to [0,1] per resource type
- $4.\,$ Generate duration targets from CPM critical path analysis
- 5. Split multi-mode projects into separate instances per mode

B.3 Benchmark Dataset Preprocessing

PSPLIB preprocessing.

- 1. Parse $.\,\mathtt{sm}$ and $.\,\mathtt{rcp}$ files for activity networks
- 2. Extract precedence relations from successor lists
- 3. Normalize resource requirements to [0,1] per resource type
- 4. Generate duration targets from CPM critical path analysis
- 5. Split multi-mode projects into separate instances per mode
- 6. Filter instances: remove projects with <10 or >150 activities for consistent evaluation
- 7. Compute graph features: betweenness centrality, clustering coefficient, path lengths

NASA93 preprocessing.

- 1. Load dataset from PROMISE repository format
- 2. Handle categorical cost drivers:
 - RELY, DATA, CPLX, TIME, STOR, VIRT, TURN: ordinal encoding (VL=1, L=2, N=3, H=4, VH=5, XH=6)
 - Development mode: one-hot encoding (organic, semi-detached, embedded)
- 3. Normalize continuous features (KLOC, effort) via log-transform then z-score
- 4. Construct surrogate graph:
 - Phase nodes: Requirements, Preliminary Design, Detailed Design, Code/Unit Test, Integration, System Test
 - Sequential edges: Requirements \rightarrow Prelim Design \rightarrow Detailed Design \rightarrow Code \rightarrow Integration \rightarrow System Test
 - Feature broadcasting: Project-level cost drivers replicated to all phase nodes
 - Phase-specific features: Weight distribution based on typical effort allocation (e.g., 15% requirements, 20% design, 35% coding, 20% integration, 10% testing)
- 5. Target variable: effort (person-months) distributed across phases using historical ratios
- 6. Train/test split: stratified by development mode

COCOMO II preprocessing.

- 1. Load dataset with 22 cost drivers plus KLOC
- 2. Handle scale factors (PREC, FLEX, RESL, TEAM, PMAT): ordinal encoding (VL=1 to XH=6)
- 3. Handle effort multipliers (17 factors): similar ordinal encoding
- 4. Missing values: mode imputation for categoricals, median for KLOC
- 5. Graph construction (hybrid approach):
 - Lifecycle phases: 6 nodes (Requirements, Architecture, Design, Implementation, Test, Deployment)
 - Component modules: When available from documentation, add module nodes within Implementation phase
 - Edges: Sequential between phases; parallel within Implementation for modules; feedback edge from Test to Implementation (rework)
- 6. Reuse percentage: Model as reduction in Code node work quantity
- 7. Target: Effort and schedule distributed via COCOMO II formulas

Desharnais preprocessing.

- 1. Load 81 software projects from financial institutions
- 2. Features: TeamExp (experience), ManagerExp, YearEnd, Length, Transactions, Entities, PointsAdjust, Language, PointsNonAdjust
- 3. Encode Language: one-hot (Cobol, Natural, PL/I, C, Pascal, etc.)
- 4. Normalize experience features (years) via min-max scaling
- 5. Graph construction (simplified chain):
 - 4 phase nodes: Analysis, Design, Coding, Testing
 - Sequential edges with uniform transition
 - All project features broadcast to phases
- 6. Target: Effort (person-hours) split equally across phases due to lack of detailed data
- 7. Remove 3 outlier projects with effort $> 3\sigma$ from mean

B.4 Additional Visualizations

Learning curves. Figure 10 shows training and validation loss progression for different models.

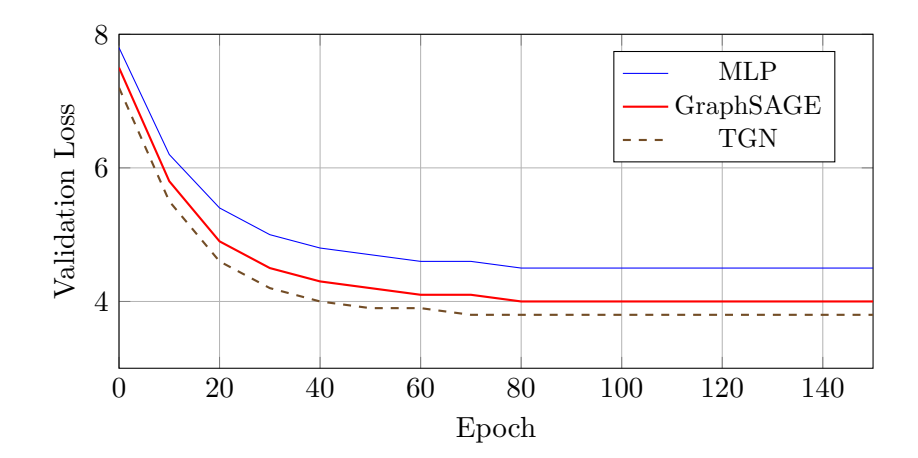


Figure 10: Learning curves: validation loss vs. training epoch. GraphSAGE converges faster than MLP (80 vs. 100 epochs) and achieves lower final loss. TGN shows similar convergence with slightly better final performance.

Error distribution analysis. Figure 11 shows the distribution of prediction errors for different models.

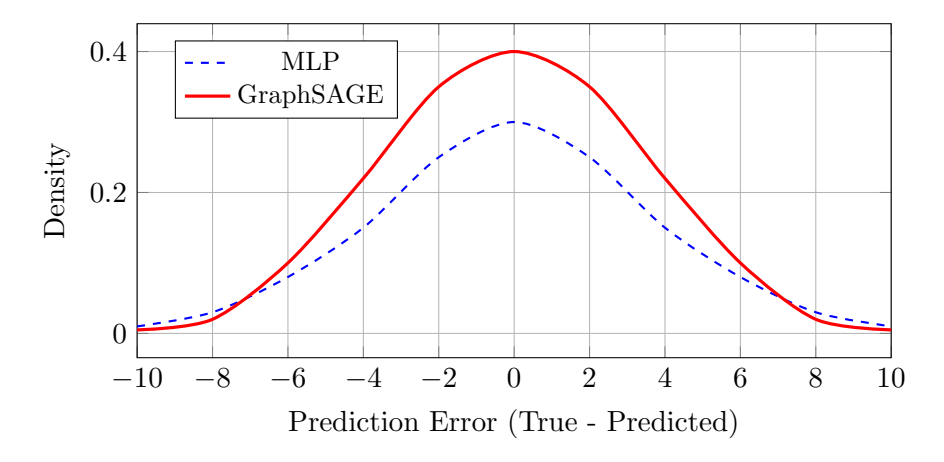


Figure 11: Error distribution: GraphSAGE shows tighter distribution (narrower, taller peak) indicating more consistent predictions with fewer large errors.

Feature embedding visualization. We use t-SNE to visualize learned node embeddings from the final GNN layer, colored by activity characteristics.

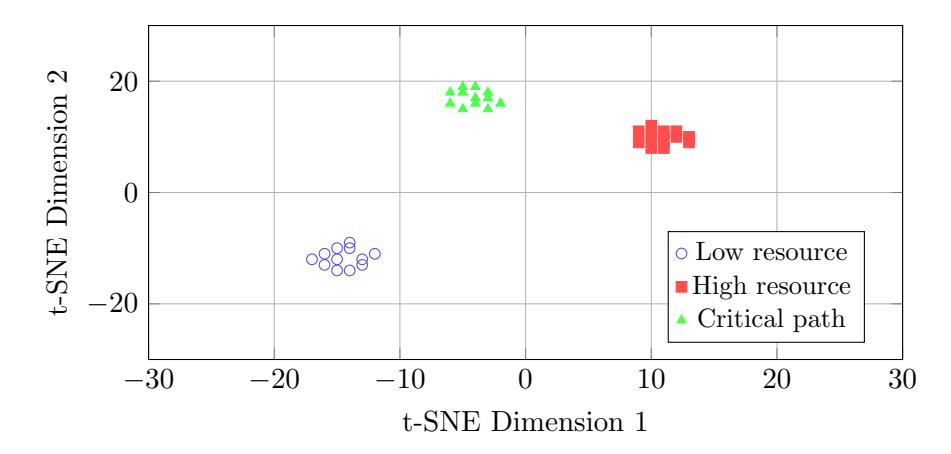


Figure 12: t-SNE visualization of learned embeddings: activities cluster by resource intensity and critical path membership, indicating the model has learned meaningful representations of project structure.

C Notation Reference

Table 23 provides a comprehensive reference for mathematical notation used throughout the paper.

Table 23: Mathematical notation reference.

Symbol	Definition
Project Structure	
G = (V, E)	Project network: directed acyclic graph with nodes V (ac-
	tivities) and edges E (precedence)
${\cal P}$	Set of all paths from source to sink in G
p^*	Critical path (longest path)
$\mathcal{N}(i)$	Neighborhood of node i
$\deg^{in}(i), \deg^{out}(i)$	In-degree and out-degree of activity i
Resources	
${\cal R}$	Set of all resources in the project
$A_i \subseteq \mathcal{R}$	Resources assigned to activity i
$R_{i,j}$	Efficiency of resource j on activity i (ratio of realized to
- 13	standard productivity)
$q_{i,j}$	Work quantity required from resource j for activity i
p_j^s	Standard productivity of resource j
c_{j}	Cost rate of resource j (e.g., $\$$ /hour)
μ_j, σ_j^2	Mean and variance of resource j efficiency distribution
Activities	
T_{i}	Duration of activity i (ground truth)
C_{i}	Cost of activity i (ground truth)
T_i^{est}, C_i^{est}	Planner baseline estimates
\hat{T}_i,\hat{C}_i	Model predictions
$\lambda_i \in [0, 1]$	Parallelism parameter: 1=serial, 0=fully parallel
F_{i}	Finish time of activity i under schedule
Project-Level	
$T_{ m proj}$	Project makespan (total duration)
$C_{ m proj}$	Total project cost
$T_{ m max}$	Deadline or target makespan
$C_{ m overhead}$	Fixed overhead costs
Graph Neural Net	works
$\mathbf{x}_i \in \mathbb{R}^d$	Feature vector for node i
$\mathbf{h}_i^{(\ell)} \in \mathbb{R}^{d_h}$	Hidden representation of node i at layer ℓ
K	Number of GNN layers
$W^{(\ell)}, b^{(\ell)}$	Weight matrix and bias for layer ℓ
$\sigma(\cdot)$	Nonlinear activation function (ReLU, GELU, etc.)
$\widetilde{\mathrm{AGG}}(\cdot)$	Aggregation function (mean, max, sum, etc.)
ψ_T,ψ_C	Prediction heads for duration and cost
	Continued on next nage

 $Continued\ on\ next\ page$

Table 23 – Continued from previous page

Symbol	Definition
Uncertainty	
$\sigma_{T.i}^2, \sigma_{C.i}^2$	Predicted variance (aleatoric uncertainty) for activity i
ECE	Expected Calibration Error
PI_{90}	90% prediction interval coverage
Loss Functions	
${\cal L}$	Total loss function
\mathcal{L}_{act}	Activity-level prediction loss
\mathcal{L}_{proj}	Project-level consistency loss
$\lambda_{act}, \lambda_{proj}, \lambda_{reg}$	Loss weighting hyperparameters
λ_T,λ_C	Weights for duration vs. cost objectives
au	Temperature parameter for soft-max approximations
Data and Evaluat	ion
n,p	Number of activities and resources
$ \mathcal{D} $	Dataset size (number of projects or activities)
MAE, RMSE	Mean Absolute Error, Root Mean Square Error
MAPE	Mean Absolute Percentage Error
R^2	Coefficient of determination
ρ	Spearman rank correlation or edge density

D Reproducibility Statement

We are committed to full reproducibility of our experimental results. This appendix documents all information necessary to replicate our findings.

D.1 Open Source Release

Upon publication, all materials will be publicly available at:

https://github.com/rezamirjaliliphd/RBM

The repository includes:

- Complete source code for all models and experiments
- Trained model checkpoints for all main results
- Synthetic data generator with exact parameterization
- Preprocessed benchmark datasets (where licensing permits)
- Configuration files for all reported experiments
- Evaluation scripts to reproduce tables and figures
- $\bullet\,$ Jupy ter notebooks with step-by-step tutorials
- Comprehensive documentation and API reference
- Unit tests and continuous integration setup

D.2 Dependencies and Environment

Software versions.

• Python: 3.10.12

• PyTorch: 2.1.0

• PyTorch Geometric: 2.4.0

• NumPy: 1.24.3

• Pandas: 2.0.3

 \bullet Scikit-learn: 1.3.0

• XGBoost: 2.0.0

• NetworkX: 3.1

• Matplotlib: 3.7.2

• Seaborn: 0.12.2

• CUDA: 12.1

• cuDNN: 8.9.2

Hardware specifications.

• GPU: NVIDIA GeForce RTX 4090 (24GB VRAM)

• CPU: AMD Ryzen 9 7950X (16 cores, 32 threads)

• RAM: 64GB DDR5-5600

• Storage: 2TB NVMe SSD

• Operating System: Ubuntu 22.04 LTS

Docker container. A Docker container with all dependencies pre-installed is available:

```
docker pull username/project-prediction-gnn:latest
docker run --gpus all -it -v $(pwd):/workspace \
      username/project-prediction-gnn:latest
```

D.3 Random Seeds and Determinism

All experiments use fixed random seeds for reproducibility:

- Global random seeds: {13, 29, 47, 71, 101}
- PyTorch: torch.manual_seed(seed)
- NumPy: np.random.seed(seed)
- Python: random.seed(seed)
- CUDA: torch.cuda.manual_seed_all(seed)

For exact reproducibility on CUDA:

```
torch.backends.cudnn.deterministic = True
torch.backends.cudnn.benchmark = False
```

Note: Deterministic CUDA operations may reduce performance by 10–20%.

D.4 Computational Budget

Total computational resources used:

- Synthetic experiments: \sim 120 GPU-hours
- \bullet Benchmark experiments: ${\sim}40$ GPU-hours
- Hyperparameter search: ~ 80 GPU-hours
- Ablation studies: ~ 30 GPU-hours
- \bullet Total: ${\sim}270$ GPU-hours on RTX 4090

Equivalent on other hardware (approximate):

- NVIDIA A100 (40GB): \sim 180 GPU-hours
- NVIDIA V100 (32GB): \sim 350 GPU-hours
- NVIDIA RTX 3090 (24GB): ${\sim}320$ GPU-hours

CPU-only training is feasible but 5–10× slower.

D.5 Data Availability

Synthetic data. Generated on-demand using provided code with documented random seeds. No external data required.

Benchmark datasets.

- PSPLIB: Publicly available at http://www.om-db.wi.tum.de/psplib/
- NASA93: Available in PROMISE repository at http://promise.site.uottawa.ca/SERepository/
- COCOMO II: Available from USC Center for Systems and Software Engineering
- **Desharnais**: Available in PROMISE repository

We provide preprocessed versions in standardized format with our code release.

D.6 Execution Instructions

```
Quick start (single experiment).
```

```
# Generate data
python data/synthetic_generator.py --size 200 --samples 100

# Train model
python training/train.py \
     --model graphsage \
     --config configs/graphsage_optimal.yaml \
     --seed 13

# Evaluate
```

python training/evaluate.py --checkpoint results/best_model.pt

Full reproduction.

```
# Run all experiments (takes ~12 hours on RTX 4090)
bash scripts/run_all_experiments.sh

# Generate all tables and figures
python scripts/generate_results.py --input results/ --output paper/
```

D.7 Expected Runtime

On NVIDIA RTX 4090:

- Single GraphSAGE training (size 200, 100 samples): 15 minutes
- Full synthetic experiments (all sizes, 5 seeds): 6 hours
- Benchmark experiments (4 datasets, 5-fold CV): 2 hours
- Ablation studies: 3 hours
- Active learning experiments: 1 hour

D.8 Known Issues and Limitations

- 1. CUDA non-determinism: Some CUDA operations have inherent randomness even with fixed seeds. Results may vary by $\pm 0.5\%$ across runs.
- 2. **Hardware dependency**: Training times and memory usage vary by GPU model. Batch sizes may need adjustment for GPUs with <16GB VRAM.
- 3. Numerical precision: Results may differ slightly (typically < 0.1%) between float 32 and bfloat 16/mixed precision training.
- 4. **Library versions**: Minor differences in results (†1%) may occur with different PyTorch/PyG versions due to implementation changes.
- 5. **Operating system**: Some operations (e.g., multithreading) behave differently on Windows vs. Linux, potentially affecting runtime but not results.

D.9 Verification Checklist

To verify successful reproduction:

- 1. Check that generated synthetic data statistics match reported values (Table 1 in main text)
- 2. Verify model architecture matches specifications (count parameters: GraphSAGE should have ${\sim}200\mathrm{K}$ params)
- 3. Confirm training converges to reported validation loss within 5% (Figure 10)
- 4. Check final test RMSE within 5% of reported values
- 5. Verify statistical significance tests yield p < 0.05 for all main comparisons

D.10 Contact Information

For questions or issues with reproduction:

- GitHub Issues: https://github.com/rezamirjaliliphd/RBM
- Email: rmirjalili@uh.edu

We commit to responding to reproduction inquiries within 2 weeks and maintaining the codebase for at least 5 years post-publication.

E Ethics and Broader Impact

E.1 Ethical Considerations

This research focuses on project management prediction systems with the following ethical considerations:

Intended use. The proposed framework is designed to support project managers in:

- Improving schedule and budget forecasting
- Identifying high-risk activities requiring attention
- Optimizing resource allocation decisions
- Enhancing transparency through uncertainty quantification

Potential misuse. We acknowledge potential risks:

- Overreliance on predictions: Automated forecasts may lead to complacency or reduced human oversight. We emphasize that predictions should augment, not replace, expert judgment.
- Workforce monitoring: Resource performance modeling could enable excessive surveillance. Organizations should implement predictions ethically with worker consent and transparency.
- Bias amplification: If training data reflects historical biases (e.g., systematic underestimation for certain activity types), models may perpetuate these patterns. Regular audits and bias testing are recommended.
- Gaming the system: Knowing prediction mechanisms, stakeholders might manipulate inputs to achieve favorable forecasts. Safeguards and validation against manipulation are necessary.

Mitigation strategies. We recommend:

- 1. Maintaining human-in-the-loop decision making with model predictions as advisory
- 2. Implementing fairness audits to detect and correct systematic biases
- 3. Providing uncertainty quantification alongside predictions to communicate confidence levels
- 4. Establishing governance frameworks for ethical AI use in organizations
- 5. Protecting worker privacy through anonymization and aggregation

E.2 Broader Impact

Positive impacts.

- Improved project success rates: Better predictions can reduce cost overruns and delays, benefiting organizations and society
- Resource efficiency: Optimal allocation reduces waste and environmental impact
- Scientific advancement: Open-source release enables further research and methodological improvements
- Accessibility: Free tools democratize advanced project management capabilities for small organizations

Potential negative impacts.

- **Job displacement**: Automation of forecasting tasks may reduce demand for certain project management roles
- **Increased pressure**: More accurate predictions could intensify pressure on workers to meet targets
- **Digital divide**: Organizations lacking data infrastructure may be unable to benefit, widening competitive gaps
- Environmental costs: Computational requirements have carbon footprint (estimated ~ 50 kg CO₂ for full training suite)

Societal considerations. Project management affects diverse sectors (construction, software, infrastructure, healthcare). Improved predictions could:

- Accelerate critical infrastructure projects (hospitals, schools, clean energy)
- Reduce public sector budget overruns, freeing resources for social programs
- Enable better disaster response and humanitarian project planning
- Support developing economies in building technical capacity

E.3 Limitations and Responsible Use

Users should be aware of limitations:

- 1. Models are trained on historical data and may not generalize to unprecedented situations
- 2. Predictions have inherent uncertainty; overconfidence in point estimates is dangerous
- 3. Models cannot account for all external factors (pandemics, geopolitical events, etc.)
- 4. Ethical deployment requires organizational commitment beyond technical implementation

We encourage responsible use guided by human values, organizational context, and stakeholder engagement.

This appendix provides comprehensive documentation supporting full reproducibility and responsible use of our research. For additional information, please contact the corresponding author or visit the project repository.

References

- [1] Akintola S Akintoye. Analysis of factors influencing project cost estimating practice. Construction Management & Economics, 18(1):77-89, 2000.
- [2] M Sanjeev Arulampalam, Simon Maskell, Neil Gordon, and Tim Clapp. A tutorial on particle filters for online nonlinear/non-gaussian bayesian tracking. *IEEE Transactions on Signal Processing*, 50(2):174–188, 2002.

- [3] Pablo Ballesteros-Pérez, Saïd Elamroussi, and María C González-Cruz. Tender price forecasting with machine learning: Application to construction projects. *Automation in Construction*, 99:13–29, 2019.
- [4] Jacek Blazewicz, Jan Karel Lenstra, and AHG Rinnooy Kan. Scheduling subject to resource constraints: classification and complexity. *Discrete Applied Mathematics*, 5(1):11–24, 1983.
- [5] David M Blei, Alp Kucukelbir, and Jon D McAuliffe. Variational inference: A review for statisticians. *Journal of the American Statistical Association*, 112(518):859–877, 2017.
- [6] Barry Boehm, Chris Abts, A Winsor Brown, Sunita Chulani, Bradford K Clark, Ellis Horowitz, Ray Madachy, Donald J Reifer, and Bert Steece. Cocomo ii model definition manual, 2000.
- [7] Stephen Boyd and Lieven Vandenberghe. *Convex optimization*. Cambridge University Press, 2004.
- [8] Tyson R Browning. Design structure matrix extensions and innovations: a survey and new opportunities. *IEEE Transactions on Engineering Management*, 63(1):27–52, 2016.
- [9] Hongyun Cai, Vincent W Zheng, and Kevin Chen-Chuan Chang. Active learning for graph embedding. In *Proceedings of the 23rd ACM SIGKDD International Conference on Knowledge Discovery and Data Mining*, pages 79–88, 2017.
- [10] Min-Yuan Cheng and Nhat-Duc Hoang. Evolutionary fuzzy hybrid neural network for dynamic project success assessment in construction industry. Automation in Construction, 118:103283, 2020.
- [11] Min-Yuan Cheng, Hsing-Chih Tsai, and Wei-Shuo Hsieh. Artificial intelligence for construction duration forecasting. *Automation in Construction*, 133:104049, 2022.
- [12] Kyunghyun Cho, Bart Van Merriënboer, Caglar Gulcehre, Dzmitry Bahdanau, Fethi Bougares, Holger Schwenk, and Yoshua Bengio. Learning phrase representations using rnn encoderdecoder for statistical machine translation. Proceedings of the 2014 Conference on Empirical Methods in Natural Language Processing (EMNLP), pages 1724–1734, 2014.
- [13] Jean-Marc Desharnais. Software cost estimation: A neural network approach. In *Proceedings* of the 5th International Forum on COCOMO and Cost Modeling, 1989.
- [14] Salah E Elmaghraby. On the fallacy of averages in project risk management. European Journal of Operational Research, 165(2):307–313, 2005.
- [15] Samuel ElSayegh, Hazim El-Mounayri, and Ali Al Haddad. Construction cost prediction using machine learning and statistical modeling. *Journal of Construction Engineering and Management*, 147(1):04020148, 2021.
- [16] Steven D Eppinger and Tyson R Browning. Design structure matrix methods and applications. MIT press, 2012.
- [17] Wenqi Fan, Yao Ma, Qing Li, Yuan He, Eric Zhao, Jiliang Tang, and Dawei Yin. Graph neural networks for social recommendation. *The World Wide Web Conference*, pages 417–426, 2019.
- [18] Bent Flyvbjerg. What you should know about megaprojects and why: An overview. *Project Management Journal*, 45(2):6–19, 2014.
- [19] Bent Flyvbjerg and Alexander Budzier. The iron law of megaproject management: the first law of wing walking. *California Management Review*, 64(3):5–29, 2022.
- [20] David N Ford and John D Sterman. Modeling project success through recursive evaluation of task contingencies and strategic objectives. *System Dynamics Review*, 23(1):1–35, 2007.
- [21] Linton C Freeman. A set of measures of centrality based on betweenness. *Sociometry*, 40(1):35–41, 1977.
- [22] Justin Gilmer, Samuel S Schoenholz, Patrick F Riley, Oriol Vinyals, and George E Dahl. Neural message passing for quantum chemistry. *International Conference on Machine Learning*, pages 1263–1272, 2017.
- [23] Walter J Gutjahr, Christine Strauss, and Edeltraud Wagner. Multi-objective optimization for scheduling and inspection planning of stochastic network projects. *European Journal of Operational Research*, 227(2):293–301, 2013.

- [24] Miklos Hajdu. Handbook of construction scheduling: principles, methodology, and types. Springer, 2015.
- [25] Will Hamilton, Zhitao Ying, and Jure Leskovec. Inductive representation learning on large graphs. In *Advances in Neural Information Processing Systems*, volume 30, 2017.
- [26] Sepp Hochreiter and Jürgen Schmidhuber. Long short-term memory. *Neural Computation*, 9(8):1735–1780, 1997.
- [27] John Hu and Yan Zhang. Bayesian network learning for data-driven design. ASCE-ASME Journal of Risk and Uncertainty in Engineering Systems, 2(2):021002, 2016.
- [28] Mohamad Y Jaber and Maurice Bonney. Learning curves for processes generating defects requiring reworks. *European Journal of Operational Research*, 159(3):663–672, 2004.
- [29] Rudolph E Kalman. A new approach to linear filtering and prediction problems. *Journal of Basic Engineering*, 82(1):35–45, 1960.
- [30] Kyungki Kang and Jenny Lin. Deep learning-based construction project scheduling visualizer. In *Proceedings of the 36th International Symposium on Automation and Robotics in Construction*, pages 795–802, 2019.
- [31] Donald L Keefer and Samuel E Bodily. Three-point approximations for continuous random variables. *Management Science*, 29(5):595–609, 1983.
- [32] James E Kelley and Morgan R Walker. Critical-path planning and scheduling. *Operations Research*, 9(3):296–320, 1961.
- [33] Alex Kendall and Yarin Gal. What uncertainties do we need in bayesian deep learning for computer vision? Advances in Neural Information Processing Systems, 30, 2017.
- [34] Homayoun Khamooshi and Hamed Golafshani. Earned value project management and scheduling: a perspective to project performance. Cost Engineering, 56(2):12–22, 2014.
- [35] Byung-Cheol Kim and Kenneth F Reinschmidt. Monte carlo simulation-based analysis of dynamic risk for project scheduling. *Journal of Construction Engineering and Management*, 137(8):594–602, 2011.
- [36] Thomas N Kipf and Max Welling. Semi-supervised classification with graph convolutional networks. In *International Conference on Learning Representations (ICLR)*, 2017.
- [37] Tord Kjellstrom, Ingvar Holmer, and Bruno Lemke. Mathematical models of occupational heat exposure and worker productivity. *Industrial Health*, 47(6):528–536, 2009.
- [38] George B Kleindorfer. Stochastic networks and the extreme value distribution. *Operations Research*, 19(7):1600–1615, 1971.
- [39] Rainer Kolisch and Arno Sprecher. Psplib-a project scheduling problem library: Or software-orsep operations research software exchange program. European Journal of Operational Research, 96(1):205–216, 1997.
- [40] Rainer Kolisch and Arno Sprecher. Psplib project scheduling problem library. http://www.om-db.wi.tum.de/psplib/, 2023. Accessed: 2024-01-15.
- [41] Walt Lipke. Schedule is different. The Measurable News, 31(1):10-15, 2003.
- [42] Peter ED Love and Jane Matthews. Systems information modelling: Theoretical and research development. *Automation in Construction*, 99:1–9, 2019.
- [43] John M Lyneis and David N Ford. System dynamics for market forecasting and structural analysis. System Dynamics Review, 17(1):3–25, 2001.
- [44] Kenneth R MacCrimmon and Charles A Ryavec. An analytical study of the pert assumptions. Operations Research, 12(1):16–37, 1964.
- [45] Donald G Malcolm, John H Roseboom, Charles E Clark, and Willard Fazar. Application of a technique for research and development program evaluation. *Operations Research*, 7(5):646–669, 1959.
- [46] Tim Menzies, Dan Port, Zhihao Chen, and Jairus Hihn. The nasa software cost estimation dataset. PROMISE Repository, University of Ottawa, 2005.

- [47] Hazhir Rahmandad and John Sterman. Heterogeneity and network structure in the dynamics of diffusion: Comparing agent-based and differential equation models. *Management Science*, 54(5):998–1014, 2008.
- [48] Emanuele Rossi, Ben Chamberlain, Fabrizio Frasca, Davide Eynard, Federico Monti, and Michael Bronstein. Temporal graph networks for deep learning on dynamic graphs. In *ICML Workshop on Graph Representation Learning*, 2020.
- [49] Franco Scarselli, Marco Gori, Ah Chung Tsoi, Markus Hagenbuchner, and Gabriele Monfardini. The graph neural network model. *IEEE Transactions on Neural Networks*, 20(1):61–80, 2009.
- [50] Michael Schlichtkrull, Thomas N Kipf, Peter Bloem, Rianne Van Den Berg, Ivan Titov, and Max Welling. Modeling relational data with graph convolutional networks. In *European Semantic Web Conference*, pages 593–607. Springer, 2018.
- [51] D Sculli. The completion time of pert networks. *Journal of the Operational Research Society*, 34(2):155–158, 1983.
- [52] Burr Settles. Active learning literature survey. University of Wisconsin-Madison Department of Computer Sciences Technical Report, 2009.
- [53] Martin Skutella. Approximation algorithms for the discrete time-cost tradeoff problem. *Mathematics of Operations Research*, 23(4):909–929, 1998.
- [54] Hyojoo Son, Changwan Kim, and Changwon Kim. Data-driven framework to predict productivity in steel fabrication. *Automation in Construction*, 124:103568, 2021.
- [55] Ashish Vaswani, Noam Shazeer, Niki Parmar, et al. Attention is all you need. In *Advances in Neural Information Processing Systems*, volume 30, 2017.
- [56] Petar Veličković, Guillem Cucurull, Arantxa Casanova, Adriana Romero, Pietro Lio, and Yoshua Bengio. Graph attention networks. In *International Conference on Learning Representations*, 2018.
- [57] David Vose. Risk analysis: a quantitative guide. John Wiley & Sons, 3rd edition, 2008.
- [58] Xiao Wang, Houye Ji, Chuan Shi, Bai Wang, Yanfang Ye, Peng Cui, and Philip S Yu. Heterogeneous graph attention network. *The World Wide Web Conference*, pages 2022–2032, 2019.
- [59] Mathias Wauters and Mario Vanhoucke. Understanding and applying machine learning: a guide for asset managers. Expert Systems with Applications, 64:193–201, 2016.
- [60] Terry M Williams. The need for new paradigms for complex projects. *International Journal of Project Management*, 17(5):269–273, 1999.
- [61] Terry M Williams. Modelling complex projects. Wiley, 2002.
- [62] Da Xu, Chuanwei Ruan, Evren Korpeoglu, Sushant Kumar, and Kannan Achan. Inductive representation learning on temporal graphs. In *International Conference on Learning Representations*, 2020.
- [63] Barbaros Yet, Anthony Constantinou, Norman Fenton, Martin Neil, Eike Luedeling, and Keith Shepherd. A bayesian network framework for project cost, benefit and risk analysis with an agricultural development case study. *Expert Systems with Applications*, 60:141–155, 2016.
- [64] Cheng Zhang, Song Wang, Yuqi Wu, and Bin Xu. Graph neural network for software defect prediction. In *IEEE International Conference on Software Analysis*, Evolution and Reengineering (SANER), pages 140–150. IEEE, 2021.